NBER WORKING PAPER SERIES

ADDRESSING PARTIAL IDENTIFICATION IN CLIMATE MODELING AND POLICY ANALYSIS

Charles F. Manski
Alan H. Sanstad
Stephen J. DeCanio

Working Paper 28449
http://www.nber.org/papers/w28449

NATIONAL BUREAU OF ECONOMIC RESEARCH
1050 Massachusetts Avenue
Cambridge, MA 02138
February 2021

Dr. Sanstad's work was partially supported by the National Science Foundation through the Center for Robust Decision-Making on Climate and Energy Policy at the University of Chicago. We would like to thank the research team of Professor Elizabeth Moyer, Department of Geosciences, University of Chicago, for providing CMIP5 model output, and Valentyn Litvin, Department of Economics, Northwestern University, for his technical review. We have benefitted greatly from the comments of Robert Pindyck and Robert Rosner. The views expressed herein are those of the authors and do not necessarily reflect the views of the National Bureau of Economic Research.

Addressing Partial Identification in Climate Modeling and Policy Analysis
Charles F. Manski, Alan H. Sanstad, and Stephen J. DeCanio
NBER Working Paper No. 28449
February 2021
JEL No. D81,Q54,Q58

ABSTRACT

Numerical simulations of the global climate system provide inputs to integrated assessment modeling for estimating the impacts of greenhouse gas mitigation and other policies to address global climate change. While essential tools for this purpose, computational climate models are subject to considerable uncertainty, including inter-model "structural" uncertainty. Structural uncertainty analysis has emphasized simple or weighted averaging of the outputs of multi-model ensembles, sometimes with subjective Bayesian assignment of probabilities across models. However, choosing appropriate weights is problematic. To use climate simulations in integrated assessment, we propose instead framing climate model uncertainty as a problem of partial identification, or "deep" uncertainty. This terminology refers to situations in which the underlying mechanisms, dynamics, or laws governing a system are not completely known and cannot be credibly modeled definitively even in the absence of data limitations in a statistical sense. We propose the min-max regret (MMR) decision criterion to account for deep climate uncertainty in integrated assessment without weighting climate model forecasts. We develop a theoretical framework for cost-benefit analysis of climate policy based on MMR, and apply it computationally with a simple integrated assessment model. We suggest avenues for further research.

Charles F. Manski
Department of Economics
Northwestern University
2211 Campus Drive
Evanston, IL 60208-2600
and NBER
cfmanski@northwestern.edu

Alan H. Sanstad
1849 Shattuck Avenue Apt. 407
Berkeley, CA 94709
USA
alansanstad@gmail.com

Stephen J. DeCanio
Department of Economics (emeritus)
University of California at Santa Barbara
stephen.decanio@gmail.com

1. Introduction

Computational modeling of the global climate system provides a foundation for estimating the effects of greenhouse gas (GHG) mitigation and other policies on global climate change. Climate models project the future path of the climate as a function of trajectories of anthropogenic GHG emissions and other inputs.[*] They are used to predict the climatic and other impacts of altering emission trajectories by means of various GHG reduction policies, which in turn supports analysis of how to address the climate change problem.

Climate models aim to represent the immensely complicated climate system in a tractable manner. Scientific understanding of the climate, as developed over decades of research by many scholars around the world, is at this point remarkable in its scope and depth. It remains, however, incomplete, and continues to evolve. Hence, the construction and use of climate models entail choices by modelers regarding model elements that are not fully specified by physical theory or exactly determined by empirical evidence. Over time, different sets of choices have yielded different climate models

Researchers have sought to understand and quantify the uncertainties in climate models and the predictions that they yield. One primary approach is multi-model ensemble (MME) analysis of inter-model structural choices (1). This paper offers a perspective on the uncertainties MME analysis seeks to address, from the vantage point of econometrics, decision theory, and energy policy analysis. We frame climate model uncertainty as a problem of *partial identification*, or "deep uncertainty." This terminology refers to situations in which the underlying mechanisms governing a system are not completely known and cannot be credibly modeled definitively even in the absence of data limitations in a statistical sense.

[*] This paper focuses on coupled atmospheric, ocean, and land-surface models; we follow the custom of using the term "climate model" to refer to these coupled systems.

The predictions yielded by a partially identified model of a system are set-valued rather than exact or probabilistic. Thus, partial identification generates what is referred to in various disciplines as "ambiguity," "model uncertainty," "deep uncertainty," or "epistemic uncertainty." Study of partial identification has origins mainly in econometrics, which applies statistical methods to study economic phenomena. In this field, partial identification refers to circumstances in which the probability distribution governing a stochastic system is not completely known theoretically and its unknown aspects cannot be fully learned empirically even in the absence of data limitations in the sense of statistical imprecision. In the limit case where these unknown aspects can be fully learned empirically given sufficient data, the probability distribution is said to be *point identified* or simply *identified*.

The fundamental mathematical and physical theory underlying computational climate modeling is not based on probability distributions, but rather comprises a set of deterministic nonlinear partial differential equations describing large-scale atmospheric dynamics. However, due to incomplete knowledge of other physical processes and differences in ways to represent them numerically, multiple climate models have been developed around the world and are currently in use, each reflecting different but credible choices in model design and implementation. Existing models yield different projections of the global climate even with broadly-harmonized input assumptions. Put differently, neither a "consensus" climate model nor quantitative climate projections can be definitively specified with current knowledge. These inter-model differences are referred to as reflecting "structural" uncertainty. We show how this can be framed in terms of partial identification or deep uncertainty.

This paper applies partial-identification thinking to climate modeling in two ways. First, we argue on decision-theoretic grounds against the prevalent practice in climate modeling of computing simple or weighted averages of predictions across models considered in MME analysis. Computation of simple averages of predictions assumes that equal weight should be given to each model, an assumption lacking a compelling foundation (2). But determining appropriate weights is challenging, for reasons including the weak link between metrics of model validity and predictive skill (1). Some researchers have attempted to motivate computation of weighted averages as an exercise in Bayesian judgment, the weights

expressing subjective probabilities that particular models represent truth (3). However, it may be difficult to judge the credibility of the subjective probability distribution used. Rather than compute averages of, or assigning probability distributions to, predictions across models, partial identification analysis would present the *set* of predictions yielded by model ensembles as the starting point for decision-making, foregoing an attempt to reduce the set to a point through averaging.

Second, we use classical ideas in decision theory to show how these ensemble outputs can be applied directly in policy applications of climate modeling, specifically the *min-max* (4) and *min-max regret* (5) decision rules. In decision problems in general, min-max reflects the principle of preparing for the worst case. In the climate context, it would entail making policy decisions, such as carbon abatement levels, using the most "pessimistic" climate model in an ensemble – the one projecting the highest temperature changes. Min-max regret (MMR) uses multi-model information in a more nuanced way. If a climate policy maker selects one model from an ensemble and chooses, say, an emissions abatement path that is optimal for that model according to some economic metric, the economic penalty, or regret, is the excess cost of that abatement path if a different model is actually the correct one. That is, regret measures the potential sub-optimality of policies relative to climate models. The MMR rule is to choose a policy that minimizes the maximum regret, or largest degree of sub-optimality, across the climate model ensemble. [†]

MMR has been applied in several policy areas, including criminal justice (6) and public health (7). It has been used in computational modeling of energy and climate policy in a number of studies (8-12). (Cai (13) reviews this research). The present paper complements this previous work in several ways. The paper is aimed in part at climate modelers and other researchers who are non-specialists in economics but interested in the policy applications of climate modeling. Our approach is primarily conceptual rather than computational. We emphasize the partial identification paradigm and its suitability for framing structural uncertainty in climate models. We provide a theoretical discussion of MMR for climate policy, to highlight the basic idea in non-computational form. We then present a deliberately simple numerical

[†] The other primary approach to studying climate model uncertainty is Perturbed Physics Ensemble (PPE) analysis of parametric uncertainty. *Mutatis mutandis*, the concepts and methods discussed in this paper can also be applied to understanding PPEs from a decision perspective.

integrated assessment example of MMR applied to carbon abatement policy, in order to illustrate the method in a transparent way.

In what follows, Section 2 discusses the theory of partial identification as developed in econometrics and describes how climate model uncertainties can be framed in this way. Section 3 discusses technical aspects of structural uncertainties in climate modeling as a partial identification problem. Section 4 turns to decision-making under partial identification, providing background and discussing the min-max and min-max regret decision rules. Section 5 develops a numerical example illustrating their application to the problem of choosing dynamic carbon abatement policies that optimally balance abatement costs and climate economic damages. The paper ends with a summary and concluding remarks.

2. Partial Identification in Econometrics and Climate Modeling

Econometrics is the term used by economists to describe study of the logic of empirical inference. Whatever the field of science may be, the logic of empirical inference is summarized by the relationship: *assumptions* + *data* → *conclusions*. Data alone do not suffice to draw useful conclusions. Inference requires assumptions that relate the data to a question of interest. Holding fixed the available data, a fundamental difficulty of empirical research is deciding what assumptions to maintain.

2.1. Identification and Statistical Inference

Economists and many other researchers use sample data to learn about theoretically unknown aspects of the mechanisms that govern stochastic systems. Empirical research confronts problems of statistical imprecision and identification problems. Statistical theory characterizes the inferences that can be drawn by observing a finite sample of outcomes generated by a system. Identification analysis studies inferential difficulties that persist even when sample size grows without bound. The distinction between identification and statistical inference, first formalized by Koopmans (14), has long been central to the field of econometrics.

A simple example of statistical imprecision occurs when one observes a random sample of outcomes generated by a stationary system and uses this sample average to estimate the mean outcome that the system produces. Statisticians typically measure imprecision of the estimate by its variance, which decreases to zero as sample size increases. The famous "Laws of Large Numbers" imply that imprecision vanishes as sample size increases to infinity.

Identification problems encompass the spectrum of issues that are sometimes called *non-sampling errors* or *data-quality problems*. These issues cannot be resolved by amassing so-called "big data." They may be mitigated by collecting better data, but not by merely collecting more data.

A simple example of an identification problem is generated by measurement errors. Suppose that a stationary system generates a random sample of outcomes, but one observes these outcomes with error. Increasing sample size adds new observations, but it also yields further measurement errors. If one has incomplete knowledge of the process creating measurement errors and cannot collect better data that are error-free, one cannot precisely learn the system mean outcome as sample size increases to infinity.

2.2. Point and Partial Identification

For most of the twentieth century, econometricians studying inference commonly thought of identification as a binary event – a parameter of a model is either point-identified or it is not. Empirical researchers combined available data with assumptions that yield point identification and they reported point estimates of model parameters. Economists recognized that point identification often requires strong assumptions that are difficult to motivate, but they saw no other way to perform inference.

Yet there is enormous scope for fruitful inference using weaker and more credible assumptions that partially identify objects of interest. A parameter in a probabilistic model is *partially identified* if the sampling process and maintained assumptions reveal that the object lies in a set, called the *identification region* or *identified set*, that is smaller than the logical range of possibilities but larger than a single point. Sample estimates of partially identified objects generically are set-valued.

To illustrate, suppose economic theory posits that there are positive parameters $a, b,$ and c such that $Y = (a * c) * X + b + \varepsilon.$ Given a random sample of observations of pairs (X, Y), the product $d = a * c$ can be estimated by the method of least squares if it is known that ε has mean zero conditional on X. Statistical imprecision regarding d vanishes as sample size increases. However, absent additional assumptions, all that can be inferred empirically about a and c is that they lie in the set of all pairs of positive real numbers such that $a * c = d.$ That is, these parameters are partially identified, with the identification region defined by this identity.

Part of the modern literature on partial identification in econometrics focuses on the identification problems generated by imperfect data quality, including measurement error and missing data. Part focuses on identification of structural econometric models used to describe human behavior and interactions. Manski (15, 16), Tamer (17), and Molinari (18) provide in-depth reviews of the literature at different technical levels and with different emphases. Section 1 in the Supporting Information (SI) provides a brief history and some key references.

Whatever the specific subject under study, a common theme runs through the literature. One first asks what available data combined with relatively weak and highly credible assumptions reveal about the population of interest. One then studies the identifying power of stronger assumptions that still aim to retain acceptable credibility, keeping in mind a principle called (ref. 15, p. 1):

> *The Law of Decreasing Credibility*: The credibility of inference decreases with the strength of the assumptions maintained.

This principle implies that researchers face a dilemma as they decide what assumptions to maintain: Stronger assumptions yield inferences that may be more powerful but less credible.

This approach to inference makes clear the conclusions one can draw in empirical research without imposing untenable assumptions. It establishes a domain of consensus among researchers who may hold disparate beliefs about what assumptions are appropriate. Partial identification analysis also makes plain

the limits to credible inference. When identification regions turn out to be large, researchers should face up to the fact that the available data and acceptable assumptions do not support inferences as tight as they might like to achieve.

2.3. Partial Identification of Climate Models

One might think that econometrics and climate modeling are so different that econometric methodology would have little if any application to climate modeling. In this sub-section we explain why the ideas of partial identification do, in fact, apply to climate models and can serve to frame and interpret their uncertainties.

First, research in both domains faces broadly similar identification problems due to data imperfections. Climate data that might have been available in principle may have measurement errors or be missing in practice, especially data documenting climate dynamics prior to the existence of modern instrumentation. Moreover, climate data in counterfactual settings is unavailable in principle. We cannot observe what climate change would have occurred over the past century if the trajectory of anthropogenic GHG emissions had differed from its actual path.

Second, research in both domains faces the problem of modeling a complex system. The climate system comprises many different physical processes and mechanisms occurring at a range of spatial and temporal scales. Designing and implementing a climate model requires many choices regarding the underlying architecture, the methods of numerical approximation, solution technique, which physical processes to include as model components, and how to represent these processes (19). Climate model structural uncertainty arises from incomplete scientific understanding of physical phenomena, limitations of quality and quantity of empirical data available to fit models, and the need to make approximations for computational tractability.

With respect to underlying scientific principles, all general circulation models of the climate are based on a set of five deterministic equations governing atmospheric variables including temperature, pressure, humidity, and wind flow (20). These so-called “primitive equations” instantiate first-principle

laws of physics; they include partial differential equations describing a form of the classical conservation laws of momentum, mass, and energy.

However, the highly complex and nonlinear nature of the climate system makes it inevitable that the computational models used to represent it are subject to a degree of irreducible imprecision (21). Although the basic set of primitive equations is common across models in a theoretical sense, the exact way in which the equations are rendered in a particular model is subject to numerous practical choices of implementation, including choice of coordinate system, discretization approach, and numerical solutions. In addition, climate models differ in the details of which physical processes are selected for inclusion – i.e., the overall strategy used to simplify the climate into a tractable form for modeling – and how they are represented. The multiplicity of models and inter-model variations of the quantitative outputs they generate are generally referred to as reflecting "structural" uncertainty (22, 23, 24, 25).

It is important to note that this is not an exhaustive description of uncertainty in climate modeling, nor would it be if parametric uncertainty were also taken into account. The factors just discussed are "known unknowns" – they have been explicitly determined to be sources of uncertainty. By contrast, "unknown unknowns" are also presumptively present – it cannot be assumed that the models encompass all physical processes affecting the climate to an extent that is policy relevant.

To summarize, the present state of science, modeling methods, and empirical knowledge are not such that the climate system can be uniquely represented in mathematical or computational form. Nor can climate dynamics be predicted deterministically or stochastically – one can only predict a range of possible trajectories (26). Thus, we see an underlying correspondence between econometric and climate models with respect to structural uncertainty, making the concept of partial identification applicable to climate modeling.

In the following sections we elaborate on this perspective and show how it can be applied to climate change-related policy decision-making.

3. Partial identification and multi-model ensemble analysis

At the beginning of the paper we introduced the terminology of climate model "ensembles." It is difficult to vary a given model's components such as sub-grid process representations (much less numerical integration schemes) to assess the effects of variations in structural components on the model's performance. Thus, to quantify and analyze structural uncertainty, sets of models are run to study how the different structural choices across models affect the outputs across the set. This is "multi-model ensemble (MME)" analysis, which we discuss next.

3.1. MMEs background

MMEs are based on model intercomparison projects in which the characteristics and performance of individual and multiple models are analyzed. First conducted in the 1980s (27), such projects have since proliferated and greatly increased in scope and detail. Most MME analyses have been generated in the Coupled Model Intercomparison Project (CMIP), which began in the 1990s and has thus far completed five studies (28, 29). These studies examine the individual and collective ability of models to simulate the current and historical climate, analyze the factors driving model behavior and inter-model differences, and provide a means of assessing changes in model performance over time (30).

The performance of climate models in simulating present and past climate has been gauged by various metrics based on the mean squared error of differences between model outputs, or "fields," and their observed counterparts, such as global mean temperature and precipitation (31). Comparison of model performance based on such metrics has been conducted using CMIP MMEs of historical simulations (32).

The CMIP and other intercomparison projects have been part of a substantial international research effort to develop and improve the models. Advances in computational hardware and software have also been critical. The models have been refined and improved in a number of ways, including the ability to simulate key aspects of the historical climate.

Nevertheless, there continue to be shortcomings in the models' accuracy and precision (1). There are non-trivial biases and uncertainties in particular fields across models that have persisted through development cycles (33, 34, 35). As noted previously, structural uncertainty arises from the fact that theory and evidence do not completely constrain design and implementation choices such as which sub-grid processes to include, at what levels of detail. When assessing model performance in historical simulations, there are multiple model fields for which performance metrics can be defined and quantified, and modelers have not been able to develop a single metric that effectively captures all the dimensions of interest (24). Because the relative accuracies of different models can depend on which field is measured, it has not proven possible to unambiguously rank models with respect to performance or to identify a "best" model using historical climate information (31). The extent of structural uncertainty can be gauged by the fact that there are currently several dozen different modeling groups around the world, each running one or more versions of its own model (36).

Abramowitz et al. (37) take the view that different models can be thought of as representing different "working hypotheses" about how to best represent the details of the structure and dynamics of the climate. Parker (26) characterizes the climate modeling community's acceptance of multiple, co-existing models as "model pluralism," with different models seen as complementary. In the language of the present paper, the climate models are only partially identified.

3.2. MME projections of future climate

Model pluralism has generally been maintained in MME studies of the future climate, in that the sets of models used in specific studies have usually been determined simply by which modeling teams choose to participate, a procedure Knutti (2) describes as "model democracy." That available models are not assessed or screened for inclusion essentially reflects the unavailability of reliable, agreed-upon criteria for doing so: If *ab initio* structural uncertainty (partial identification) cannot be resolved through standard evaluation and performance intercomparison, there are no obvious grounds to omit particular models from climate projection studies. Nevertheless, some modelers and climate scientists believe that there are

important shortcomings in model democracy for projective MME analysis (2). Developing better approaches has been the focus of considerable research on narrowing model selection criteria and/or finding ways of assessing candidate models according to some informational criterion.

Most of this work is closely tied to, or part of, a broader long-term effort to address uncertainty in MMEs of future climate. A number of methods have been developed and applied to MME uncertainty quantification and analysis, virtually all of which involve combining MME outputs into single projected climate trajectories. There appear to be two primary reasons that this form of model combination predominates: Simple averaging across models can improve accuracy relative to individual models in historical simulations (38), and modelers perceive policy-makers as requiring single projections (as functions of individual GHG emissions scenarios) for use in decision-making (26).

Simple averaging reflects model democracy. Weighted averaging is sometimes performed when it is felt that models can be ranked with respect to relative accuracy in specific fields in historical simulations (even if not overall) (39). Thus, models may be weighted along particular dimensions of policy interest, and the results then averaged.

Expanding on this approach, numerous studies have quantified MME uncertainty and combined model projections by creating multi-model probability distributions across predictions of key variables such as global temperature, and by using them to compute mean trajectories. Bayesian techniques are one approach to doing this – e.g., Smith et al. (3) and Sexton et al. (40) – building in particular on the work of Tebaldi et al. (41, 42).

As this type of work has proceeded, climate modelers and scientists and others have recognized some persistent methodological problems in combining model projections (43, 1). Regarding the finding that model averages can improve upon the predictions of individual models, Manski (44, 45) has shown that this may be the consequence of a mathematical relationship rather than an empirical result.[‡] Also,

[‡] Specifically, Jensen's Inequality implies that when mean square error or another convex loss function is used to measure predictive accuracy, the accuracy of a simple or weighted mean prediction is algebraically better than the corresponding average accuracy of individual model predictions.

model performance with respect to specific fields in historical data has not been demonstrated to imply skill in predicting climate (46), weakening the case for this approach to weighting projections.

Other issues have to do with how relationships among the models, and the selection of model ensemble subsets from the entire set of extant models, affect the informational content and quality of the ensemble results. These topics have been framed in terms of the degrees or levels of model "independence" in ensembles, although the formal meaning of "independence" has not been clear. In particular, one should be wary of conceptualizing independence in statistical terms, in the absence of a probabilistic theory of model development. As noted above, ensembles are typically assembled by convenience, in the sense that they are determined by the availability and interests of modelers. Thus, one cannot reasonably assert that any given ensemble is a random sample drawn from a population of potential models. Nor can one reasonably assert that any given ensemble adequately expresses the full range of structural uncertainty in model projections (24). Indeed, it is not known how well the world's complete set of existing climate models expresses the full range of uncertainty.

While it is inappropriate to conceptualize model independence in statistical terms, there may be good reason to think non-statistically about dependence across models. Modeling teams communicate with one another and they may, hence, influence the modeling choices that they collectively make. In fact, some models share parts of their codes (47).

As discussed by Sanderson (1), researchers are actively working on ways to address these problems. However, combining climate model ensemble outputs into single projected trajectories of the future global climate remains a challenging and unresolved problem. In the following sections we discuss how viewing model structural uncertainty in terms of partial identification facilitates an alternative approach to using MME information in climate policy and decision-making.

4. Climate policy under partial identification: Cost-benefit analysis with the min-max and min-max regret decision rules

The issues with standard approaches to defining and quantifying uncertainties in climate modeling that we have reviewed do not obviate the fact modeling is essential for developing policies to address the risks of global climate change. What is clearly the case, however, is that addressing uncertainties remains an open, and challenging, problem. Parker (48) observed that a primary rationale for using weighting or probability analysis to combine climate model outputs into single time paths of important variables appears to be modelers' perception that policy makers require uncertainty to be represented in this form to make decisions. In this section we show that, in fact, this is not the case, and that a partial identification framing of climate modeling opens the way to alternative methods for dealing with uncertainties in decision-making. We might say that these methods allow for single *decisions* to be made without needing single *inputs* from the models.

Our departure point is climate model ensemble analysis, so the models discussed in the following sections express partial identification in terms of a discrete set of climate models. As noted earlier, our analysis does not encompass the full uncertainty inherent in numerical climate simulation. By its very nature decision analysis must explicitly specify possible "states of nature," which list only known unknowns. Our goal is to advance understanding within that paradigm.

4.1. Economic uncertainty in integrated assessment modeling

Although not our focus in this paper, for the sake of context we begin with a brief discussion of uncertainty in the economic elements of quantitative climate policy analysis, which as a rule uses computational energy-economic or integrated assessment (IA) models. (This subject is discussed by Sanstad in (49)). These are, characteristically, long-run (century-scale or more) models of the global economy including the energy system and its role in economic production, and are applied to estimating the costs of policy-induced GHG emissions reductions. IA models incorporate reduced-form representations of the climate (or more generally, the carbon cycle) and its links to the economy,

particularly the climatic effects of anthropogenic GHG emissions and in turn their effects on the economy.

The development of integrated assessment models has enabled economic analysis of how the global climate and social systems interact with one another, which has played a critical role in the development of policies to reduce GHG emissions (50). IA models are subject to uncertainty not just in their representation of the climate but also in their economic assumptions (50). Examples arise in highly-aggregated IA models in which the direct economic costs of climate change and those of GHC abatement are both represented explicitly, so that trade-offs between emissions reduction and reduced climate change-induced economic losses can be assessed. The paradigmatic example is Nordhaus's DICE (Dynamic Integrated Climate Economy) model, the most influential IA model of the last several decades (51).

In DICE and models based on it, the economic losses from climate change are represented in terms of "damage functions" that give the decreases in world-wide output resulting from increases in mean global temperature, as a proportional reduction or in dollar terms. It is recognized that these functions have uncertain theoretical and empirical grounding (52).[§]

Another feature of these models is dynamic optimization by a representative decision maker, which entails discounting to quantify the present value of future economic costs and benefits. The appropriate definition and magnitude of the discount rate is a long-standing issue in climate change economics and integrated assessment modeling (56 - 58). Controversy persists in part due to the fact that this is not only an empirical question but also a matter of theory and of ethics in regard to intergenerational equity (59).

In addition to these issues, integrated assessment model estimates of the long-run costs of large-scale GHG emissions abatement vary considerably, by some measures up to an order of magnitude (60).

[§] Some of this work has focused on improving aggregate damage functions with respect to both aggregate-level evidence and functional forms (53). Moreover, it is also the case that aggregation *per se* is a major source of this type of uncertainty, and increasing attention is being paid to empirical, statistical estimation of spatially and sectorally disaggregated climate damages (54, 55).

As evidenced by comparing these more recent estimates with examples from the 1990s (61), this uncertainty has persisted over several decades of model development

While improving estimates of the economic impacts of climate change is an active area of research, uncertainty persists. Damage functions in aggregate models continue to be debated, and model-based abatement cost estimates continue to proliferate but are not converging. Because our focus is partial identification of *climate* models and its implications for decision-making, this paper limits formal analysis of economic uncertainties to sensitivity analysis with respect to the exogenous economic parameters governing abatement and damage costs. However, our decision framework can be readily applied to economic uncertainty.

4.2. A simple theoretical framework

In what follows, we consider climate policy from a cost-benefit perspective in the context of partial identification of climate models, in which emissions abatement policy is based on comparing the costs of reducing GHG emissions with the resulting benefit in terms of avoided climate change damages. The key consideration is that the decision-maker's knowledge of these benefits is subject to uncertainty arising from the partial identification. We first develop an abstract theoretical framework and then, in the following section, implement it quantitatively using a simple integrated assessment model.

Let B_t represent the state at time t of a baseline energy-economic scenario, and let $E_t^{B_t}$ be the corresponding baseline GHG emissions. Let A_t be GHG abatement actions at time t under some climate policy, measured in the same units as emissions, let $C(A_t)$ be their cost, and $E_t^{A_t}$ be the resulting net emissions. In what follows, we will slightly abuse terminology by also referring to A_t and $E_t^{A_t}$ as "paths" or "trajectories." We assume that abatement paths are chosen from some space of feasible paths.

Emissions paths are used as inputs to a climate model *M*. We focus on the global mean temperatures projected by M as a function of these paths. Thus, let $T\left(E_t^{A_t}, M\right)$ be the global mean temperature at time

t determined by the GHG trajectory $E_t^{A_t}$ when it is simulated in the climate model *M*. Then a damage function – as discussed above – can be written as $D\left(T\left(E_t^{A_t}, M\right)\right)$.

4.2.1. Cost-benefit analysis

4.2.1.1. The min-max decision rule

For an abatement path A_t and climate model *M*, denote the associated total (abatement plus damages) cost at time *t* as $\mathbb{C}(A_t, M) \equiv C(A_t) + D\left(T(E_t^{A_t}, M)\right)$. A policy-maker seeks to minimize the present value of the cumulative cost over a planning horizon which, as is customary in the climate economics literature, we assume to be infinite. The cost-benefit climate policy problem given a particular climate model *M* is

$$\min_{A_t} \int_0^\infty \boldsymbol{C}\left(A_t, M\right) e^{-\delta t} dt, \tag{1}$$

where δ is a discount rate. In this approach, the optimal A_t is chosen with commitment at time zero – that is, it is not updated over time as new climate or cost information is obtained. As stated, (1) is a deterministic optimization problem that, under certain technical assumptions regarding the feasible abatement path space and the cost and damage functions, has a unique solution. We will assume that such conditions hold for the series of problems we describe.

Reflecting the discussion in Section 3, let $\mathbf{M} = \{M_1, \ldots, M_N\}$ be a model ensemble. We amend the damage and cost function notations to $\mathbb{C}(A_t, M_i) \equiv C(A_t) + D\left(T(E_t^{A_t}, M_i\right), \; i = 1, \ldots, N$. The hypothetical policy-maker now faces the problem of minimizing total cost while taking account of the model uncertainty. One way of approaching this problem is to assign a probability distribution or some other weighting scheme to M and minimize the expected cost. However, this strategy is unsatisfactory if one lacks a credible basis for assigning a distribution or weights.

Under a partial identification perspective, one alternative way to proceed is to apply the *min-max* decision rule, which can be characterized colloquially as "preparing for the worst." Here, the "worst" is

the model M_i that results in the highest total abatement plus damage costs. Given an abatement path A_t and associated emissions path $E_t^{A_t}$ the most costly outcome will correspond to the model that solves the problem

$$\max_i \int_0^\infty \boldsymbol{C}\left(A_t, M_i\right) e^{-\delta t} dt. \tag{2}$$

This maximum cost will vary across possible abatement paths, and the min-max decision is to select the path that solves

$$\min_{A_t} \max_i \int_0^\infty \boldsymbol{C}\left(A_t, M_i\right) e^{-\delta t} dt. \tag{3}$$

That is, the decision rule chooses the abatement policy that minimizes the total cost of abatement and damages under the most pessimistic assumption regarding the climate model.

4.2.1.2. The min-max regret decision rule

Policies chosen using the min-max criterion are conservative by design. An alternative decision rule that is applicable under conditions of partial identification but is less conservative is called *min-max regret*, which Manski and Tetenov (62) characterizes as seeking uniformly near-optimal solutions to decision problems. For each model M_i in the ensemble $\mathbf{M} = \{M_1, \ldots, M_N\}$ let $\mathbb{C}(A_t, M_i) \equiv C(A_t) + D\big(T(E_t^{A_t}, M_i)\big)$ be the associated time *t* cost with abatement and emissions paths A_t and $E_t^{A_t}$ respectively. Let $A^*_{t;M_i}$ be the abatement path that solves the problem

$$\min_{A_t} \int_0^\infty \boldsymbol{C}\left(A_t, M_i\right) e^{-\delta t} dt, \tag{4}$$

and $\mathbb{C}^*\big(A^*_{t;M_i}, M_i\big)$ be the resulting minimum cost:

$$\boldsymbol{C}^*\left(A^*_{t;M_i}, M_i\right) \equiv \min_{A_t} \int_0^\infty \boldsymbol{C}\left(A_t, M_i\right) e^{-\delta t} dt. \tag{5}$$

(Note the change in notation: Previously, $\boldsymbol{C}\left(A_t, M_i\right)$ was total cost at time *t*; now, $\boldsymbol{C}^*\left(A^*_{t;M_i}, M_i\right)$ is total discounted cost, i.e., an integral.) Now consider any other feasible trajectory A_t and its cost – not necessarily optimal – over the entire time horizon with M_i, $\int_0^\infty \boldsymbol{C}\left(A_t, M_i\right)e^{-\delta t}dt.$ The *regret* $\boldsymbol{R}\left(A_t, M_i\right)$ associated with A_t when climate model M_i is used in determining damages is the difference between its cost and the cost of the *optimal* policy associated with M_i:

$$\boldsymbol{R}\left(A_t, M_i\right) \equiv \int_0^\infty \boldsymbol{C}\left(A_t, M_i\right)e^{-\delta t}dt - \boldsymbol{C}^*\left(A^*_{t;M_i}, M_i\right). \tag{6}$$

The regret is non-negative because $\boldsymbol{C}^*\left(A^*_{t;M_i}, M_i\right)$ is the minimum cost with M_i. Regret measures the sub-optimality of A_t when temperature is determined by M_i. That is, it is the excess cost resulting from this abatement path relative to the minimal cost associated with this model.

To apply the min-max regret rule, a decision-maker first considers each feasible abatement path A_t and finds the model version that maximizes regret as defined in Equation (6), solving the problem

$$\max_{M_i} \boldsymbol{R}\left(A_t, M_i\right) = \max_{M_i} \int_0^\infty \boldsymbol{C}\left(A_t, M_i\right)e^{-\delta t}dt - \boldsymbol{C}^*\left(A^*_{t;M_i}, M_i\right). \tag{7}$$

The min-max regret solution is then to find A_t to solve the problem

$$\min_{A_t}\max_{M_i} \boldsymbol{R}\left(A_t, M_i\right) = \min_{A_t}\max_{M_i} \int_0^\infty \boldsymbol{C}\left(A_t, M_i\right)e^{-\delta t}dt - \boldsymbol{C}^*\left(A^*_{t;M_i}, M_i\right). \tag{8}$$

This discussion highlights the fact that, in any application, MMR requires an explicit criterion to measure the differences in social welfare between optimal and sub-optimal outcomes. For example, applying the technique to analyze policies that entail exogenously-set "caps" on GHG emissions would necessitate measurement of the social cost of exceeding those caps.

5. A numerical example

In this section we describe a computational implementation of the min-max regret (MMR) framework described above. We present a simple integrated assessment model defining an optimal control problem that formalizes the dynamic economic trade-off between emissions abatement and reduced damages from emissions-caused temperature increases. We also contrast the results of applying the MMR criterion with those obtained with the min-max decision rule.[**]

5.1. A simple integrated assessment model

5.1.1. Emissions and temperature

In the previous section we represented the link between carbon emissions, in the form of a trajectory $E_t^{A_t}$, and projected global mean temperature T_t, as a functional relationship based on a climate model *M*: $T_t \equiv T\left(E_t^{A_t}, M\right)$, where $E_t^{A_t}$ are net emissions at time *t* when baseline emissions B_t are reduced by abatement A_t, and are used to project temperature using *M*. For quantitative analysis, we now simplify this representation by adapting the approach of Matthews et al. (64) to summarize the long-term relationship between aggregate carbon emissions and global mean temperature. Using a combination of modeling and observational data analysis, these researchers showed that the ratio of temperature increase to *cumulative* emissions, the "carbon-climate response (CCR)," is roughly constant over decades up to several centuries. We use the CCR to capture the influence of emissions on temperature. (This approach is further discussed in NAS (65) and Cline (66).

Let $\mathbf{E}_t^{A_t}$ be cumulative emissions between an initial time 0 and time *t* given a net emissions path $E_t^{A_t}$

$$\mathbf{E}_t^{A_t} = \int_0^t E_s^{A_s} ds. \tag{9}$$

[**] Our model is similar to that of Goulder and Mathai (63), which was adapted to min-max regret analysis of carbon abatement policy by Cai and Sanstad (11). Rezai and van der Ploeg (12) developed a more complex integrated assessment model and applied it to max-min and min-max regret analysis of climate analysis under uncertainty, using temperature projections from several different IA models.

Let *m*(*M)* be the CCR associated with a climate model *M*. Then the Matthews *et al.* approximation of global mean temperature projected by *M* when it is driven by $E_t^{A_t}$ is

$$\begin{aligned} T_t &= T\left(E_t^{A_t}, M\right) \\ &= m(M)\int_0^t E_s^{A_s} ds = m(M)\mathbf{E}_t^{A_t}. \end{aligned} \tag{10}$$

Slightly amending our notation from the previous section, we will use the parameter *m* to characterize the models being compared. Different models might in principle have the same *m*, but this is not the case for the six we examine here. Thus, we can write the model-projected temperature as $T_t = T\left(E_t^{A_t}, m\right)$.

5.1.2. Costs and damages

We assume that the functions for abatement cost and climate damage at time *t* are quadratic:

$$\begin{aligned} C(A_t) &= \frac{1}{2}\alpha A_t^2 \\ D(T_t) &= \frac{1}{2}\beta\left(m\mathbf{E}_t^{A_t}\right)^2 = \frac{1}{2}\beta m^2(\mathbf{E}_t^{A_t})^2. \end{aligned} \tag{11}$$

The quadratic is a convenient and tractable functional form; in the present case, it enables us to solve our optimization model in closed form (see below). The shape of the damage function has been controversial in climate economics. Nordhaus and Moffat (53) conducted a comprehensive survey of empirical damage estimates in the literature and conducted their own estimations; their preferred specification was quadratic.

With $T_t = T\left(E_t^{A_t}, m\right) = m\mathbf{E}_t^{A_t}$, the total cost at time *t* is

$$\begin{aligned} \boldsymbol{C}\left(A_t, m\right) &\equiv C(A_t) + D\left(T\left(E_t^{A_t}, m\right)\right) \\ &= \frac{1}{2}\alpha A_t^2 + \frac{1}{2}\beta m^2(\mathbf{E}_t^{A_t})^2. \end{aligned} \tag{12}$$

5.1.3. Optimization

In the abstract framework of Section 4.2, any constraints that might be imposed on the optimizations were implicit. In optimal control problems, the key type of constraint specifies the dynamic relationship between the decision variable and the "state" variable – here $\mathbf{E}_t^{A_t}$ – as an ordinary differential equation. We write the cost-minimization problem for a given climate model as

$$\begin{aligned} &\min_{A_t} \int_0^\infty \frac{1}{2}\left(\alpha A_t^{\,2} + \beta T_t^{\,2}\right) e^{-\delta t} dt \\ &\quad \text{subject to} \\ &\frac{d}{dt}\mathbf{E}_t^{A_t} = E_t^{A_t} = B_t - A_t \\ &T_t = m\mathbf{E}_t^{A_t} \\ &\mathbf{E}_0^{A_t} = \mathbf{E}_0, \end{aligned} \tag{13}$$

where the last expression defines an initial condition for cumulative emissions. Solving (13) yields the abatement path $A_{t,m}^*$ that minimizes the present (discounted) values of abatement costs plus climate damages subject to the relationships among emissions, temperature, and damages. Conceptually, this path makes the optimal trade-off over time between abatement and damages.

5.2. Calibration

5.2.1. Baseline emissions projection

We created our baseline emissions path using the "Representative Concentration Pathway (RCP) 8.5" of carbon and other emissions and atmospheric concentrations created by integrated assessment modelers circa 2010 (67). It is one of four such scenarios, each corresponding to a different level of global average watts per meter squared in 2100 that was projected in one or more IAMs (68, 69). The 8.5 watts/meter-squared pathway is the highest-warming of the RCPs, reflecting a pessimistic scenario

regarding the increase in global emissions over the 21st century; it has been used as a baseline in numerous studies.

We used the RCP 8.5 projection of annual carbon emissions (fossil and land use sources) from 2000 to 2500 in gigatons of carbon (GtC), obtained from the RCP repository at the Potsdam Institute for Climate Impact Research.[††] For a baseline emissions path approximating the projection, we fitted the following functional form to these data:

$$B_t = \left(\theta t + \frac{B_0}{\exp(\theta\varphi)} \right) \exp\left(-\theta\left(t-\varphi\right)\right), \tag{14}$$

where B_0 is 8 GtC, the RCP 8.5 emissions in 2000. The fitted parameter values are $\theta = 0.0123125$ and $\varphi = 339.565$. Further details are provided in SI Section 2.

5.2.2. Temperature projections under structural uncertainty

To calibrate temperature as a function of cumulative emissions for structural uncertainty analysis, we used outputs of six earth system models (ESMs) from CMIP5 that each projected the effects of RCP 8.5. We first computed decadal averages of the CMIP5-reported monthly surface air temperature projections from these models under RCP 8.5 for the period 1900-1909 to 2090-2099. Following Matthews et al. (64) as described above, we then calculated decade-by-decade temperature increases over this period relative to 1900-1909 as projected by each ESM, along with the corresponding decade-by-decade increases in cumulative carbon emissions in RCP 8.5. Extending the notation introduced above, denote the latter quantity as $\mathbf{E}_{Cum}^{B_t}$.

For each ESM, indexed by i = 1,…,6, we represented the relationship between temperature and cumulative net emissions as

[††] http://www.pik-potsdam.de/~mmalte/rcps/.

$$T_i = m_i \mathbf{E}_{Cum}^{B_t}. \quad (15)$$

To estimate the m_i's we fitted (15) to the decadal average time series for each model. See SI Section 2 for details.

The six models and fitted values of m_i are shown in Table 1. The range among these estimates is a simple gauge of structural uncertainty.

TABLE 1 HERE

5.2.3. Economic parameters

We derived low, median, and high estimates of the abatement cost parameter α from Dietz and Venmans (70), who summarized global marginal abatement costs as a percent of global economic output as documented in the *IPCC Fifth Assessment Report*. Because these costs were derived from energy-economic and integrated assessment model analyses that assumed a 5% discount rate, we used this value exclusively. For the central value of the damage cost parameter β we used Nordhaus's and Moffat's (53) central estimate from their preferred (quadratic) specification and estimation of the climate damage function. We also specified low and high values for sensitivity analysis. The values for these parameters are presented in Table 2.

TABLE 2 HERE

5.3 Analytical and numerical solutions

Using standard methods, the model is solved in closed form analytically and the numerical solution is computed using the Mathematica (71) software; details are presented in SI Section 3. The results are optimal abatement paths $A_{t;m_i}^*$ and minimum costs

$$\begin{aligned} \boldsymbol{C}^*\left(A_{t;m_i}^*, m_i\right) &= \min_{A_t} \int_0^\infty \boldsymbol{C}\left(A_t, m_i\right) e^{-\delta t} dt \\ &= \min_{A_t} \int_0^\infty \frac{1}{2}\left(\alpha A_t^{\,2} + \beta T_t^{\,2}\right) e^{-\delta t} dt, \end{aligned} \quad (16)$$

subject to the constraints in (13).[‡‡] Details are presented in SI Section 3.

5.4. Min-Max Regret under structural uncertainty

We begin with an example of how regrets are calculated, in the case that FIO is the correct model and with the median and central values of α and β, respectively. Our analysis assumes that the state space of possible real worlds includes only those represented by the six models. That is, it excludes the possibility that all six models are wrong. In principle, the calculations could be done with a larger state space that has more distinct models. However, we reiterate the point made earlier: No finite ensemble can enable analysis of the "unknown unknowns" of climate modeling.

The first row of Table 3 shows $\boldsymbol{C}^{*}\left(A^{*}_{t;m_i}, m_i\right),\ i = 1,\mathsf{K}\ ,6,$ the minimum total discounted abatement costs plus climate damages, associated with the optimal trajectory $A^{*}_{t;m_i}$ for each model for the median α and central β parameter case. We assign the indices i in the order in which the models are listed in Table 1; that is according to ascending values of the CCR parameter.

To explain the second row, we recall the idea of a sub-optimal trajectory from Section 4.3, here assuming for the sake of discussion that FIO (i = 3) is the correct model. For legibility, we again amend our previous notation: Let $A^{*}_{t,i\neq 3}$ be the optimal trajectory for one of the models other than FIO and $E\left(A^{*}_{t,i\neq 3}\right)$ be the net emissions at time t when this trajectory is used to reduce emissions from the baseline B_t, i.e., $E\left(A^{*}_{t,i\neq 3}\right) = B_t - A^{*}_{t,i\neq 3}$. We write the resulting cumulative emissions path as

$$\begin{aligned}\mathbf{E}_t\left(A^{*}_{t,i\neq 3}\right) &= \int_0^t E\left(A^{*}_{s,i\neq 3}\right) ds \\ &= \int_0^t \left(B_s - A^{*}_{s,i\neq 3}\right) ds.\end{aligned} \tag{17}$$

[‡‡] Under our assumptions, the necessary conditions are also sufficient, and the model will have unique solutions with the parameters we use.

Now consider using this emissions path to project temperature with the FIO CCR, m_3:

$$\begin{aligned} T_t &= T\left(E\left(A^*_{t,i\neq 3}\right)\right) \\ &= m_3 \int_0^t E\left(A^*_{s,i\neq 3}\right) ds \\ &= m_3 \mathbf{E}_t\left(A^*_{t,i\neq 3}\right). \end{aligned} \tag{18}$$

That is, $T_t = m_3 \mathbf{E}_t\left(A^*_{t,i\neq 3}\right)$ is the temperature path when the optimal trajectory for a *different* model is used with the FIO CCR. In turn, we calculate the time *t* abatement costs associated with $A^*_{t,i\neq 3}$ and climate damages associated with $m_3 \mathbf{E}_t\left(A^*_{t,i\neq 3}\right)$:

$$\begin{aligned} \boldsymbol{C}\left(A^*_{t,i\neq 3}, m_3\right) &= C\left(A^*_{t,i\neq 3}\right) + D\left(T\left(E\left(A^*_{t,i\neq 3}\right)\right)\right) \\ &= \frac{1}{2}\alpha\left(A^*_{t,i\neq 3}\right)^2 + \frac{1}{2}\beta m_3{}^2\left(\mathbf{E}_t\left(A^*_{t,i\neq 3}\right)\right)^2. \end{aligned} \tag{19}$$

The present value of these costs is then

$$\begin{aligned} \boldsymbol{C}_{PV}\left(A^*_{t,i\neq 3}, m_3\right) &= \int_0^\infty \left(C\left(A^*_{s,i\neq 3}\right) + D\left(T\left(E\left(A^*_{s,i\neq 3}\right)\right)\right)\right) e^{-\delta s} \\ &= \int_0^\infty \left(\frac{1}{2}\alpha\left(A^*_{s,i\neq 3}\right)^2 + \frac{1}{2}\beta m_3{}^2\left(\mathbf{E}_s\left(A^*_{s,i\neq 3}\right)\right)^2\right) e^{-\delta s}. \end{aligned} \tag{20}$$

Equation (20) displays the sub-optimality we have referred to: It is a cost, but not the *optimal* cost, using the FIO model to project temperature. These sub-optimal costs for the models $i = 1, 2, 4, 5, 6$ comprise the second row of Table 3.

TABLE 3 HERE

The last row of the Table presents the associated regrets, the differences between the sub-optimal costs and the optimal (minimum) cost with the FIO model:

$$\boldsymbol{R}\left(A^*_{t,i\neq 3}, m_3\right) = \boldsymbol{C}_{PV}\left(A^*_{t,i\neq 3}, m_3\right) - \boldsymbol{C}^*\left(A^*_{t,m_3}, m_3\right), \tag{21}$$

for i = 1,2,4,5,6. As discussed in Section 4.3, these are the *post hoc* losses when a decision-maker implements the optimal abatement policy assuming that one of the models other than FIO is correct, but FIO is in fact the correct model.

The full set of regrets across the six models for the median α and central β case is shown in Table 4:

$$\boldsymbol{R}\left(A^*_{t,i\neq j}, m_j\right) = \boldsymbol{C}_{PV}\left(A^*_{t,i\neq j}, m_j\right) - \boldsymbol{C}^*\left(A^*_{t,m_j}, m_j\right),$$

$i, j = 1,\ldots,6.$ The rows are regrets with respect to the models listed at the left, with the FIO row values equal to those in the last line of Table 3. For example, the number in the second row, fourth column (0.01266) is the regret from using the Hadley model to perform the optimization when the correct model is the BCC. The min-max regret (MMR) solution across entire the table is in shown bold italics, and occurs when FIO is the correct model and MIROC used instead for the optimization.

TABLE 4 HERE

Note that the values in each row form a "U" shape with respect to the zero value for the correct model for the row. In the rows with the three lowest CCRs – GFDL, BCC, and FIO – the maximum regret occurs with the MIROC model, while for the rows with the three highest CCRs – Had, IPSL, and MIROC – it occurs with the GFDL. This is intuitive given the relative magnitudes of the various CCRs.

This calculation of the MMR solution assumes that the action space (that is, the set of feasible abatement paths) includes only the six abatement paths that are optimal under one of the models. Thus, it takes the action space to be the set of "best response" paths. More generally, society could consider abatement paths that are not optimal under any of the six models. Even if the state space comprises only the six models, it is possible that the MMR path will be one that is not optimal in any state. Thus, Table 4 gives a constrained MMR solution. Finding the unconstrained MMR abatement path would be a much more complex computational problem.

To explore the sensitivity of the MMR to the economic parameters, we calculated nine tables for the nine α, β pairs. Table 5 summarizes the results, showing the MMR for each combination of α and β. For

all these parameter pairs the MMR occurs with FIO as the model selected for optimization and MIROC as the incorrect model.

TABLE 5 HERE

It is interesting to see that the MMR is increasing in β for each value of α, that is, the greater the sensitivity of climate damages to cumulative carbon, the greater the regret for using an incorrect ESM. The MMR is also increasing in α for the central and high values of β, but not for the low value.

A sensitivity analysis of the model with respect to the economic parameters is presented in SI Section 3; its results and the data in Table 4 allow us to compare the MMR and min-max decision rule outcomes. The sensitivity analysis shows that the MIROC model yields the highest cost optimal solution for all α, β pairs – that is, if MIROC correctly embodies the CCR, the outcome is the worst using our optimization model. It is natural to ask, what will the cost turn out to be if MIROC is correct, but another model is chosen? The answer is of course the set of regrets associated with MIROC. Comparing the MIROC and FIO rows in Table 4, we see that the MIROC regrets are in some cases higher and in some cases lower than those for FIO. But its maximum regret (0.06558, when GFDL is chosen but MIROC is correct) is greater than FIO's maximum regret (0.01749). The difference between the two can be interpreted as the potential cost of using the min-max rather than the MMR decision rule with this optimization model.

6. Conclusion

Computational climate modeling is a challenging endeavor. Over decades, the efforts of many modelers around the world have yielded steady progress in model development. The models enable policy-makers to analyze the long-range consequences of societal decisions about energy production and use. However, the complexities of the climate system and computational difficulties generate *structural*

uncertainty. A consequence is that a number of distinct models have been developed over time and are currently in use,

Taking account of this uncertainty in integrated assessment modeling and other policy applications has with few exceptions relied on climate model weighting of one kind or another, including Bayesian probabilistic analysis. The shortcomings of these weighting schemes are known and well-documented in the technical literature. As an alternative, we have proposed a *partial identification* framing and cost-benefit analysis of climate policy using the *min-max regret criterion.* We have provided a theoretical treatment of min-max regret decision-making under structural uncertainty, and a simple numerical integrated assessment example. The min-max regret criterion offers a rationally grounded way to deal with structural uncertainty, and our results establish that the partial identification approach is a promising avenue for further development of computational modeling for climate policy.

There are several ways this work could be extended. MMR analysis of joint parametric and structural climate model uncertainty could be conducted by explicitly distinguishing the two in the link between cumulative emissions and temperature. Of particular interest is MMR analysis of the types of economic uncertainties we discussed, both in their own right and jointly with climate model uncertainty. Such research could greatly enhance the capacity of decision-makers to address this most challenging of environmental problems.

References

1. B. M. Sanderson, Uncertainty Quantification in Multi-Model Ensembles. *Oxford Research Encyclopedia of Climate Science,* Online, October (2018).

2. R. Knutti, The end of model democracy? *Climatic Change* 102, 395-404 (2010).

3. R. L. Smith, C. Tebaldi, D. Nychka, L. O. Mearns, Bayesian Modeling of Uncertainty in Ensembles of Climate Models. *J. Am. Stat. Assoc* 104, 485, 97-116 (2009).

4. A. Wald, *Statistical Decision Functions* (New York: Wiley, 1950).

5. L. J. Savage, The Theory of Statistical Decision. *J. Am. Stat. Assoc.* 46, 55-67 (1951).

6. Manski, C., "Search Profiling with Partial Knowledge of Deterrence," The Economic Journal, 116, F385-F401 (2006).

7. Manski, C., "Vaccination with Partial Knowledge of External Effectiveness," *Proc. Natl. Acad. Sci. U.S.A.* 107, 3953-3960 (2010).

8. R. Loulou, A. Kanudia, Minimax regret strategies for greenhouse gas abatement: methodology and application. *Oper. Res. Lett.* 25, 5, 219-230 (1999).

9. T. Iverson, Communicating Trade-offs amid Controversial Science: Decision Support for Climate Policy. *Ecol. Econ.* 77, 74-90 (2012).

10. D. Anthoff, R. Tol, Climate policy under fat-tailed risk: an application of FUND. *Ann. Oper. Res.*, Springer, 220, 1, 223-237, September (2014).

11. Y. Cai, A. H. Sanstad, Model uncertainty and energy technology policy: The example of induced technical change. *Comput. Oper. Res.* 66, 362-373 (2016).

12. A. Rezai, F. v. d. Ploeg, Climate policies under climate model uncertainty: Max-min and min-max regret. *Energ. Econ.* 68, 4-16 (2017).

13. Y. Cai, Computational Methods in Environmental and Resource Economics. *Ann. Rev. Resour. Econ.* 11, 59-82 (2019).

14. T. Koopmans, Identification Problems in Economic Model Construction. *Econometrica* 17, 125-144 (1949).

15. C. Manski, *Partial Identification of Probability Distributions* (New York: Springer-Verlag, 2003).

16. C. Manski, *Identification for Prediction and Decision* (Cambridge: Harvard University Press, 2007a).

17. E. Tamer, Partial Identification in Econometrics. *Annu. Rev. Econ.* 2, 167-195 (2010).

18. F. Molinari, Microeconomics with partial identification. *Handbook of Econometrics (*Elsevier, 2020).

19. K. McGuffie, A. Henderson-Sellers, *A Climate Modelling Primer – Third Edition.* (Chichester, England: John Wiley & Sons, 2005).

20. CCSP, *Climate Models: An Assessment of Strengths and Limitations*. A Report by the U. S. Climate Change Science Program and the Subcommittee on Global Change Research [Bader D. C., C. Covey, W. J. Gutowski Jr., I. M. Held, K. E. Kunkel, R. L. Miller, R. T. Tokmakian and M. H. Zhang (Authors), Department of Energy, Office of Biological and Environmental Research, Washington, D. C., USA, 124 pp. (2008).

21. J. C. McWilliams, Irreducible imprecision in atmospheric and oceanic simulations. *P. Natl. Acad. Sci. USA* 104, 21, 8709-8713 (2007).

22. T. N. Palmer, G. J. Shutts, R. Hagedorn, F. J. Doblas-Reyes, T. Jung, M. Leutbecher, Representing Model Uncertainty in Weather and Climate Prediction. *Annu. Rev. Earth Pl. Sc.* 33, 163-193 (2005).

23. D. A. Stainforth, M. R. Allen, E. R. Tredger, L. A. Smith, Confidence, uncertainty and decision-support in climate predictions. *Phil. Trans. R. Soc. A* 365, 2145-2161 (2007).

24. R. Knutti, R. Furrer, C. Tebaldi, J. Cermak, G. A. Meehl, Challenges in Combining Projections from Multiple Climate Models. *J. Climate* 23, 15 May, 2739-2758 (2010).

25. W. S. Parker, Ensemble modeling, uncertainty and robust predictions. *WIRES Clim. Change* 4, 213-223 (2013).

26. W. S. Parker, Understanding Pluralism in Climate Modeling. *Found. Sci.* 11, 349-368 (2006).

27. S. J. Lambert, G. J. Boer, Atmosphere-ocean heat fluxes and stresses in general circulation models. *Atmos. Ocean* 27:4, 692-715 (1989).

28. G. A. Meehl, G. J. Boer, C. Covey, M. Latif, R. J. Stouffer, The Coupled Model Intercomparison Project. *B. Am. Meteorol. Soc. (BAMS)* 81, 2, 313-318 (2000).

29. G. A. Meehl, C. Covey, B. McAvaney, M. Latif, R. J. Stouffer, Overview of the Coupled Model Intercomparison Project. *B. Am. Meteorol. Soc. (BAMS),* January, 89-93 (2005).

30. K. E. Taylor, R. J. Stouffer, G. A. Meehl, An Overview of CMIP5 and the Experimental Design. *B. Am. Meteorol. Soc. (BAMS*)*,* April, 485-498 (2012).

31. P. J. Gleckler, K. E. Taylor, C. Doutriaux, Performance metrics for climate models. *J. Geophys. Res.* 113, D06104 (2008).

32. M. Collins, B. B. B. Booth, B. Bhaskaran, G. R. Harris, J. M. Murphy, D. M. H. Sexton, M. J. Webb, Climate model errors, feedbacks, and forcings: a comparison of perturbed physics and multi-model ensembles. *Clim. Dynam.* 36, 1737-1766 (2011).

33. C. Wang, L. Zhang, S-K. Lee, L. Wu, C. R. Mechoso, A global perspective on CMIP5 climate model biases. *Nat. Clim. Change* 4, March, 201-205 (2014).

34. A. Gainusa-Bogdan, F. Hourdin, A. K. Traore, P. Braconnot, Omens of coupled model biases in the CMIP5 AMIP simulations. *Clim. Dynam.* 51, 2927-2941 (2018).

35. B. J. Soden, W. D. Collins, D. R. Feldman, Reducing uncertainties in climate models. *Science* 361, 6400, 27 July, 326-327 (2018).

36. World Climate Research Programme (WCRP), Overview [of] CMIP6 Experimental Design and Organization. https://www.wcrp-climate.org/wgcm-cmip/wgcm-cmip6 (2016).

37. G. Abramowitz, N. Herger, E. Gutmann, D. Hammerling, R. Knutti, M. Leduc, R. Lorenz, R. Pincus, G.A. Schmidt, Model dependence in multi-model climate ensembles: weighting, sub-selection and out-of-sample testing. *Earth Syst. Dynam. Discussions* (2018). Available at https://doi.org/10.5194/esd-2018-51.

38. T. Reichler, J. Kim, How Well Do Coupled Models Simulate Today's Climate? *B. Am. Meteorol. Soc. (BAMS*), March, 303-311 (2008).

39. F. Giorgi, L. O. Mearns, Probability of regional climate change based on the Reliability Ensemble Averaging (REA) method. *Geophys. Res. Lett.* 30, 12, 1629 (2003).

40. D. M. H. Sexton, J. M. Murphy, M. Collins, M. J. Webb, Multivariate probabilistic projections using imperfect climate models part I: outline of methodology. *Clim. Dynam.* 38, 2513-2542 (2012).

41. C. Tebaldi, L. Mearns, D. Nychka, R. Smith, Regional probabilities of precipitation change: a Bayesian analysis of multimodel simulations. *Geophys. Res. Lett.* 31, L24, 213 (2004).

42. C. Tebaldi, R. L. Smith, D. Nychka, L. O. Mearns, Quantifying uncertainty in projections of regional climate change: A Bayesian approach to the analysis of multimodel ensembles. *J. Climate* 18, 10, 1524-1540 (2005).

43. C. Tebaldi, R. Knutti, The use of the multi-model ensemble in probabilistic climate projections. *Phil. Trans. R. Soc. A,* 365, 2053-2075 (2007).

44. C. Manski, Interpreting and combining heterogeneous survey forecasts. In M. Clements and D. Hendry, Eds., *Oxford Handbook on Economic Forecasting*, 457-472 (2011).

45. C. Manski, Interpreting Point Predictions: Some Logical Issues. *Found. Trends Accounting* 10, 2-4, 238-261 (2016).

46. G. Flato, J. Marotzke (Coordinating Lead Authors), "Evaluation of Climate Models," in Stocker, T. F., et al, Eds., *Climate Change 2013: The Physical Science Basis. Contribution of Working Group I to the Fifth Assessment Report of the Intergovernmental Panel on Climate Change*, Cambridge University Press (2013).

47. R. Knutti, D. Masson, A. Gettelman, Climate model genealogy: Generation CMIP5 and how we got there. *Geophys. Res. Lett.* 40, 1194-1199 (2013).

48. W. S. Parker, Whose Probabilities? Predicting Climate Change with Ensembles of Models. *Philos. Sci.* 77, 5, 985-997 (2010).

49. A. H. Sanstad, Energy-economic policy modeling. AIP Conference Proceedings **1924**, 020011 (2018); https://doi.org/10.1063/1.5020291

50. J. Weyant, Some Contributions of Integrated Assessment Models of Global Climate Change. *Rev. Env. Econ. Policy* 11, 1, Winter, 115-137 (2017).

51. W. D. Nordhaus, Climate Change: The Ultimate Challenge for Economics. *Am. Econ. Rev*. 109 (6), 1991-2014 (2019).

52. R. Pindyck, Climate Change Policy: What Do the Models Tell Us? *J. Econ. Lit.* 51, 3, September, 860-872 (2013).

53. W. D. Nordhaus, A. Moffat, A Survey of Global Impacts of Climate Change: Replication, Survey Methods, and a Statistical Analysis. NBER Working Paper No. 23646 (2017).

54. S. Hsiang et al., Estimating economic damage from climate change in the United States. *Science* 356, 1362-1369, 30 June 2017.

55. M. Auffhammer, Quantifying Economic Damages from Climate Change. *J. Econ. Perspect.* 32, 4, Fall, 33-52 (2018).

56. F. Ackerman, S. J. DeCanio, R. B. Howarth, K. Sheeran, Limitations of integrated assessment models of climate change. *Climatic Change* 95, 297-315 (2009).

57. D. A. Weisbach, C. R. Sunstein, Climate Change and Discounting the Future: A Guide for the Perplexed. 27 *Yale L. & Pol'y Rev.* 433 (2009).

58. R. Pindyck, The Use and Misuse of Models for Climate Policy. *Rev. Env. Econ. Policy* 11, 100-114 (2017).

59. P. Dasgupta, Discounting climate change. *J. Risk Uncertainty* 37, 2/3, Special Issue on Discounting Dilemmas (December), 141-169 (2008).

60. L. Clarke, L., K. Jiang, *Assessing Transformation Pathways*. In O. Edenhofer et al., eds., *Climate Change 2014: Mitigation of Climate Change. Contribution of Working Group III to the Fifth Assessment Report of the Intergovernmental Panel on Climate Change.* Cambridge University Press, Cambridge, United Kingdom and New York, NY, USA (2014).

61. C. Fischer, R. D. Morgenstern, Carbon Abatement Costs: Why the Wide Ranges of Estimates? *Energ. J.* 27, 2, 73-86 (2006).

62. C. Manski, A. Tetenov, Sufficient Trial Size to Inform Clinical Practice. *P. Natl. Acad. Sci. USA* 113, 10518-10523 (2016).

63. L. H. Goulder, K. Mathai, Optimal CO_2 Abatement in the Presence of Induced Technical Change. *J. Environ. Econ. Manag.* 39, 1-38 (2000).

64. H. D. Matthews, N. P. Gillett, P. A. Stott, K. Zickfeld, The proportionality of global warming to cumulative carbon emissions. *Nat. Lett.* 459, 829-832 (2009).

65. National Academies of Sciences, Engineering, and Medicine (NAS), Assessment of Approaches to Updating the Social Cost of Carbon: Phase 1 Report on a Near-Term Update. Committee on Assessing Approaches to Updating the Social Cost of Carbon, Board on Environmental Change and Society. Washington, DC: The National Academies Press, doi: 10.17226/21898 (2016).

66. W. R. Cline, Transient Climate Response to Cumulative Emissions (TCRE) As A Reduced-form Climate Model. Economics International, Inc. (2020).

67. K. Riahi et al., RCP 8.5 – A scenario of comparatively high greenhouse gas emissions. Climatic Change 109, 33-57 (2011).

68. R. H. Moss et al., The next generation of scenarios for climate change research and assessment. Nature 463, 747-756, doi: 10.1038/nature08823 (11 February 2010).

69. M. Meinshausen et al., The RCP greenhouse gas concentrations and their extensions from 1765 to 2300. Climatic Change 109, 213-241, DOI 10.1007/s10584-011-0156-z (2011).

70. S. Dietz, F. Venmans, Cumulative carbon emissions and economic policy: In search of general principles. J. Environ. Econ. Manag. 96, 108-129 (2019).

71. Wolfram Research, Inc., *Mathematica 12*. Champaign, IL (2020).

Table 1. Carbon-climate response estimates – six earth system models, CMIP5 temperature projections under RCP 8.5

Earth system model	Fitted m_i under RCP 8.5 (degrees Celsius per teraton carbon)
GFDL-ESM-2G - Geophysical Fluid Dynamics Laboratory Earth System Model version 2G	1.573
BCC-CSM-1 - Beijing Climate Center Climate System Model version 1.1	1.864
FIO-ESM - FIO-ESM - First Institute of Oceanography Earth System Model	1.937
Had-GEM2-ES - Hadley Global Environmental Model 2 - Earth System	2.286
IPSL-CM5A-MR - Institut Pierre Simon Laplace Coupled Model 5A - Medium Resolution	2.361
MIROC-ESM - Model for Interdisciplinary Research on Climate - Earth System Model	2.438

Table 2. Values of economic parameters used for calibration

Abatement cost parameter α (Fractional GDP lost per GtC abated)		**Climate damage cost parameter β (Fractional GDP loss per degrees Celsius increase)**	
Low	0.000078	Low	0.014
Median	0.000125	Central (Nordhaus & Moffat 2017)	0.018
High	0.0002	High	0.022

Table 3. Example of regrets calculation – with FIO the correct model, median α and central β

	Model					
Calculations	GFDL	BCC	FIO	Had	IPSL	MIROC
Optimal values for each model (assuming it is correct)	0.293	0.381	0.4029	0.509	0.531	0.554
Sub-optimal values (if other models' optimal paths are used but FIO is the correct model)	0.413	0.4033	-	0.412	0.416	0.420
Regrets: Sub-optimal values minus FIO optimum	0.01059	0.0004	0	0.0088	0.01274	0.01749

Table 4. Values of regret across six ESMs, median α and central β, including Min-Max Regret solution (in bold italics)

	INCORRECT MODEL (COLUMN)						
CORRECT MODEL (ROW)	GFDL	BCC	FIO	Had	IPSL	MIROC	Row maxima
GFDL	0	0.00608	0.00939	0.03436	0.04137	0.04914	0.04914
BCC	0.00669	0	0.00039	0.01266	0.01726	0.02266	0.02266
FIO	0.01059	0.0004	0	0.0088	0.01274	***0.01749***	***0.01749***
Had	0.04357	0.01459	0.0099	0	0.00041	0.00166	0.04357
IPSL	0.05379	0.0204	0.0147	0.00042	0	0.00043	0.05379
MIROC	0.06558	0.02748	0.02071	0.00175	0.00044	0	0.06558

Table 5. Values of Min-Max Regret among six climate models across economic parameters (from the FIO/MIROC model pair in each case)

	Value of *β*		
	Low	*Central*	*High*
Value of *α*			
Low	0.01300	0.01538	0.01719
Median	0.01387	0.01749	0.02053
High	0.01312	0.01763	0.02179

Supporting Information

1. Research on Partial Identification

1.1. Partial Identification Due to Imperfect Data

A large body of research on partial identification has studied the inferential problems created by imperfect data, where imperfection can mean measurement error or missing data. Obtaining larger samples does not resolve these inferential problems. Measurement error and missing data generate identification problems, not merely statistical imprecision.

Notable early studies of partial identification with measurement error include (1) and (2). They derived sharp bounds on the slope parameter of a simple linear regressions with *errors-in-variables*; that is, white-noise measurement error in the outcome and covariate. These early findings were later extended to multiple linear regression by (3). More recent work on partial identification with measurement error has studied nonparametric inference with contaminated and corrupted sampling (4) and misclassification (5) rather than white-noise error.

Another notable early subject of study was use of knowledge of the marginal distribution of each element of a vector of random variables to partially identify the joint probability distribution of the vector or conditional distributions (6). See (7) and (8) respectively for more recent contributions to these subjects. In this body of work, the data imperfection is that one can observe each element of a vector in isolation from one another, but one lacks data on the vector in totality.

A prominent concern of econometricians has been partial identification with missing data. Early on, (9) suggested conservative analysis of surveys with missing data due to nonresponse by sample members, informally distinguishing between identification problems and those of statistical inference. Manski (10) initiated formal analysis of partial identification with missing data, determining what can be concluded about a population mean and distribution function if nothing is known about the missingness process. Many subsequent contributions have studied partial identification of various population parameters given alternative assumptions about the missingness process. Manski (11, 12) provides monograph and textbook expositions of this body of work.

Consideration of missing data problems has led to a large literature studying partial identification of treatment response, beginning with (13). Again, (11, 12) give monograph and textbook expositions of the ensuing literature. Analysis of treatment response poses a distinctive problem of missing outcome data. Studies of treatment response aim to predict the outcomes that would occur if counterfactual treatment rules were applied to a population. Treatments are mutually exclusive, so one cannot observe the outcomes that a person would experience under all treatments. At most, one can observe the outcome that a person experiences under the treatment he actually receives. The counterfactual outcomes that a person would have experienced under other treatments are logically unobservable.

1.2 Partial Identification of Structural Econometric Models

Structural econometric models place assumptions on the behavior of economic agents (consumers, firms, or governments) and on the ways that they interact with one another. These assumptions are combined with data on observed behavior and interactions to estimate model parameters. Estimated models are used to predict the choices that agents would make and the interactions that would occur in counterfactual settings. Particularly prominent are applications of the models to predict economic outcomes under counterfactual public policies.

A classic example is analysis of competitive markets. Economists assume that firm and consumer behavior are expressed by supply and demand functions. They restrict the heterogeneity of behavior across by markets through functional form assumptions (e.g., linear supply and demand) and distributional assumptions (e.g., mean independence involving so-called instrumental variables). They assume that observed transactions are market equilibria. Estimated models are used to predict the

transactions that would occur in counterfactual settings, such as under counterfactual tax and subsidy policies.

The traditional practice of applied econometrics has been to make assumptions that are strong enough to yield point identification of structural models when the assumptions are combined with data on the observable behavior of the relevant economic agents. However, the assumptions imposed are often criticized for lacking credibility.

Studies of partial identification of structural models investigate inference under weaker assumptions that may be more credible. Given such assumptions, findings distinguish models that are consistent with available data from those that are not. Thus, one narrows the scope of scientific inquiry to a set of feasible models, but one does not claim to have found a unique best model. Having determined a set of feasible models, one may use each model to predict economic outcomes in counterfactual settings. The result is a set of predictions, one for each feasible model, rather than an exact prediction or a probability distribution of predictions.

Discussion of partial identification of structural econometric models occurred as early as the 1940s, but formal analysis is more recent. Manski (13) studied partial identification of the market demand for a good when data on transactions are combined with the weak and credible assumption that demand decreases as price rises. Haile and Tamer (14) studied partial identification of the bidding rules used by participants in auctions when data on observed bids are combined with weak and credible assumptions on bidding behavior. Ciliberto and Tamer (15) studied partial identification of the rules that oligopolistic airlines use to decide whether to initiate service between specific city pairs. Manski (16, 17) studied partial identification of discrete choice models in generality and of labor supply models in particular. Barseghyan, Molinari, and Teitelbaum (18) studied partial identification of the decision rules that households use to make insurance purchases.

Studies of partial identification of structural econometric models build on the literature on partial identification due to imperfect data. In general, the data available for structural modeling suffers from measurement error and missingness. A fundamental missing data problem is that one can only observe the historical behavior of economic agents under the policies that existed at the time. The counterfactual choices that agents would have made under other policies are logically unobservable. Thus, research on structural models faces the same missing data problem that arises in analysis of treatment response.

2. Calibration

2.1. Fitting a Functional Form to RCP 8.5

The exogenous baseline emissions projection B_t driving the results of the model is the Representative Concentration Pathway (RCP) 8.5 (see main body of the text). The functional form fitted to this emissions path is given by equation (14) in the text, reproduced here as equation SI.2.1:

$$B_t = \left(\theta t + \frac{B_0}{\exp(\theta\varphi)} \right) \exp\left(-\theta\left(t-\varphi\right)\right) \qquad \text{(SI.2.1)}$$

We used Mathematica's "NonlinearModelFit" procedure specifying the Levenberg-Marquardt method (19, 20, 21). Both RCP 8.5 and the fitted version of (SI.2.1) are shown in Fig. S1.

We make no claim about any statistical properties of this curve-fitting. Our objective was solely to obtain a functional form that is analytically tractable and closely resembles the projected emissions pathway. Equation (SI.2.1) with the fitted parameters shown in the main text accomplishes this; the adjusted R^2 measure of goodness of fit is 0.927 and the fitted function exhibits the same pattern of rising and then falling gross emissions shown by RCP 8.5.

2.2. Temperature data

To estimate the simple carbon-climate response model described in Section 5.2 of the main text, we adapted the CMIP5 variable "tas" – near surface air temperature in Kelvin ("CMIP5 PCMDI standard_output.pdf," p. 19, table "CMOR Table Amon: Monthly Mean Atmospheric Fields and some Surface Fields," https://pcmdi.llnl.gov/mips/cmip5/docs/standard_output.pdf?id=54). The model output was generously provided by the research group of Professor Elizabeth Moyer, Department of Geosciences, University of Chicago. We used the projections of this variable generated by the CMIP5 earth systems models (ESMs) listed in Section 5.2. As noted there, these observations were averaged into decades starting in 1900 and ending at 2100. Information on the models, including technical references, can be found in (22).

2.3. Comparisons of Actual and Fitted Values of Temperature, Equation (15) of Main Text, Six Models Separately (Fig. S2a-f) and Together (Fig. S3).

Actual and fitted values for each model were computed using EViews11 (23). Each series for temperature and cumulative emissions had 19 observations (decadal averages), and the equation was fitted by least squares with no constant and an AR(1) process specified for the disturbance term. Fitting without specifying an autocorrelated error indicated a great deal of serial correlation of the residuals. While these estimates of the m_i were not too different from those we report, our judgment was that it was best to fit equation (15) while removing most of the autocorrelation. We make no statistical claims, but conventional measures were all indicative of a tight fit (R^2 values greater than 0.99) and the inverted AR roots were less than one.

3. Model Solutions

The current-value Hamiltonian of the simple model in Section 5 is

$$\mathbf{H} = \frac{1}{2}\alpha A_t^2 + \frac{1}{2}\beta\left(m\mathbf{E}_t^{A_t}\right)^2 + \lambda_t(B_t - A_t), \tag{SI.3.1}$$

where λ_t is an adjoint or co-state variable (a counterpart to the Lagrange multiplier in static optimization). The first-order necessary conditions are

$$\begin{aligned} \lambda_t &= \alpha A_t \\ \frac{d\lambda_t}{dt} &= \delta\lambda_t - \beta m^2 \mathbf{E}_t^{A_t} \\ \mathbf{E}_0^{A_t} &= \mathbf{E}_0 \\ \lim_{t\to\infty} e^{-\delta t}\lambda_t \mathbf{E}_t^{A_t} &= 0. \end{aligned} \tag{SI.3.2}$$

The first two equations in (SI.3.2) can be re-arranged to yield

$$\frac{dA_t}{dt} = \delta A_t - \frac{\beta m^2}{\alpha}\mathbf{E}_t^{A_t}$$
$$\frac{d\mathbf{E}_t^{A_t}}{dt} = B_t - A_t. \qquad \text{(SI.3.3)}$$

This is a two-dimensional system of linear, first-order, constant-coefficient ordinary differential equations, and can be solved in closed form with elementary methods: first a diagonalization procedure to uncouple the two equations, and second the use of an integrating factor to solve the resulting system in terms of exponential functions. Reversing the diagonalization and applying the initial and transversality conditions (the third and fourth lines in (SI.3.2)) then yields closed-form solutions for the optimal abatement path $A^*_{t;m_i}$ and cumulative carbon emissions $\mathbf{E}_t^{A_t}$ for most values of $\alpha, \beta,$ and *m*.

We obtained numerical values of α and β from Figure 3, p. 113, of (24) using the Web Plot Digitizer software (https://automeris.io/WebPlotDigitizer/).

We solved the system both by hand and using Mathematica's "DSolve" command. We also used Mathematica to solve the optimal control problem: Mathematica's "Integrate" command calculated the optimal values – minimum discounted abatement costs plus climate damages – as a function of the optimal solution paths A_t and $\mathbf{E}_t$. We present these results in the next section for the values of $\alpha, \beta,$ and *m* presented in the main text.

For both analytical and numerical solutions there is general and a special case defined by particular combinations of parameters. Our parameter values reflect the general case, but the difference between the two raises certain computational issues that we discuss in Section 3.3 below.

3.1. Numerical solutions

Fig. S4 displays the optimal abatement paths over the 21st century for each of the six ESMs as proxied by m_i, $i = 1,\ldots,6,$ for the median value of α and the central value of β. Fig. S5 shows the corresponding optimal net emissions paths ($E_t^{A_t} = B_t - A_t$ for each model) as well as the fitted baseline RCP 8.5 emissions path from equation (14) of the main text. The figures show that the optimal control model with our calibration finds fairly aggressive abatement to be optimal across the ESMs. They also show an inverse correspondence, as it were, between the geometry of these paths and the values of the CCRs: the higher the CCR, the greater is optimal abatement and the lower is optimal net emissions, with the spacing of the paths reflecting the relative differences among the numerical values of m_i.

Table S1 shows sensitivity of optimal (minimum) costs with respect to the low, middle, and high values of both α and β, for each value of m_i. The results are as would be expected: For each m_i, the optimal cost is increasing in both α and β, conversely, for each α, β pair, it is increasing in m_i. These results allow us to compare climate uncertainty and economic sensitivity in the calibrated simple model. In each row (corresponding to a value of m_i), the lowest optimal cost is in the low α, low β case, and the highest cost is in the high α, high β case. The largest row range (highest value minus lowest value) is 0.341, with the MIROC ESM. Conversely, in each column (representing an α, β pair), the lowest cost is the in first row – the GFDL model – and the highest in the last row – the MIROC model. The largest column range is 0.362, again with MIROC. That is, the magnitudes of climate uncertainty and economic sensitivity are roughly equivalent. This finding highlights the importance of taking account of *both* climate-model and economic uncertainty in quantitative studies of optimal carbon policy.

3.2. Closed form analytical solutions

3.2.1. General case: $\theta + \lambda_1 \neq 0$

Diagonalization of the system involves determining eigenvalues of the fundamental matrix

$$M = \begin{pmatrix} \delta & -\dfrac{\beta m^2}{\alpha} \\ -1 & 0 \end{pmatrix}. \tag{SI.3.5}$$

There are two, λ_1 and λ_2, which are negative and positive, respectively. We recall that the baseline emissions trajectory in our model is $B_t = \left(\theta t + \dfrac{B_0}{e^{\theta\varphi}}\right)e^{-\theta(t-\varphi)}$. The parameter condition for the general case arises in solving the diagonalized form of the equation for A_t:

$$y_1'(t) = \lambda_1 y_1(t) - \frac{\lambda_2}{(\lambda_2 - \lambda_1)}\left(\theta t + \frac{B_0}{e^{\theta\varphi}}\right)e^{-\theta(t-\varphi)},$$

or (SI.3.6)

$$y_1'(t) - \lambda_1 y_1(t) = -\frac{\lambda_2}{(\lambda_2 - \lambda_1)}\left(\theta t + \frac{B_0}{e^{\theta\varphi}}\right)e^{-\theta(t-\varphi)}.$$

Multiplying both sides by the integrating factor $e^{-\lambda_1 t}$ yields

$$e^{-\lambda_1 t}y_1'(t) - e^{-\lambda_1 t}\lambda_1 y_1(t) = -\frac{\lambda_2}{(\lambda_2 - \lambda_1)}\left(\theta t + \frac{B_0}{e^{\theta\varphi}}\right)e^{-\theta(t-\varphi)}e^{-\lambda_1 t},$$

i.e.,

$$\frac{d}{dt}\left(e^{-\lambda_1 t}y_1(t)\right) = -\frac{\lambda_2}{(\lambda_2 - \lambda_1)}\left(e^{\theta\varphi}\theta t + B_0\right)e^{-(\theta+\lambda_1)t},$$

(SI.3.7)

and

$$e^{-\lambda_1 t}y_1(t) = \int -\frac{\lambda_2}{(\lambda_2 - \lambda_1)}\left(e^{\theta\varphi}\theta t + B_0\right)e^{-(\theta+\lambda_1)t}\,dt.$$

When $\theta + \lambda_1 \neq 0$, the right-hand side of the last equation of (SI.3.7) is

$$\begin{aligned} &\int -\frac{\lambda_2}{(\lambda_2 - \lambda_1)}\left(\theta t + \frac{B_0}{e^{\theta\varphi}}\right)e^{-\theta(t-\varphi)}e^{-\lambda_1 t}\,dt = \int -\frac{\lambda_2}{(\lambda_2 - \lambda_1)}\left(e^{\theta\varphi}\theta t + \frac{B_0}{e^{\theta\varphi}}\right)e^{-(\theta+\lambda_1)t}\,dt \\ &= \frac{\lambda_2 e^{\theta\varphi}\theta}{(\lambda_2 - \lambda_1)(\theta + \lambda_1)}e^{-(\theta+\lambda_1)t}t + \frac{\lambda_2 e^{\theta\varphi}\theta}{(\lambda_2 - \lambda_1)(\theta + \lambda_1)^2}e^{-(\theta+\lambda_1)t} + \frac{\lambda_2}{(\lambda_2 - \lambda_1)(\theta + \lambda_1)}B_0 e^{-(\theta+\lambda_1)t} + C_1, \end{aligned} \tag{SI.3.8}$$

where C_1 is a constant. Substituting back into Equation (SI.3.7) and multiplying both sides by $e^{\lambda_1 t}$ yields the solution:

$$y_1(t) = \frac{\lambda_2 e^{\theta\varphi}\theta}{(\lambda_2 - \lambda_1)(\theta + \lambda_1)}e^{-\theta t}t + \frac{\lambda_2}{(\lambda_2 - \lambda_1)(\theta + \lambda_1)}\left(\frac{e^{\theta\varphi}\theta}{(\theta + \lambda_1)} + B_0\right)e^{-\theta t} + C_1 e^{\lambda_1 t} \tag{SI.3.9}$$

The solution for $y_2(t)$ is obtained analogously.

In this general case, returning to the original coordinates and setting C_1 using the initial condition for $\mathbf{E}_t$, the solutions to (SI.3.3) are of the form

$$\begin{aligned} A_t &= \mathrm{A}_1 e^{-\theta t} t + \mathrm{A}_2 e^{-\theta t} + \mathrm{A}_3 e^{\lambda_1 t} \\ \mathbf{E}_t &= \mathrm{E}_1 e^{-\theta t} t + \mathrm{E}_2 e^{-\theta t} + \mathrm{E}_3 e^{\lambda_1 t}, \end{aligned} \tag{SI.3.10}$$

where the A_i's and $\mathbf{E}_i$'s are algebraic expressions in the model parameters.

3.2.2 Special case: $\theta + \lambda_1 = 0$

The growth rates of the terms with $e^{-\theta t}$ and $e^{\lambda_1 t}$ are $-\theta$ and λ_1, respectively, and the growth rate of the terms with $e^{-\theta t} t$ is $\frac{d}{dt} \ln e^{-\theta t} t = \frac{1}{t} - \theta$, i.e., $-\theta$ asymptotically. Thus if $\theta + \lambda_1 = 0$, these growth rates coincide as $t \to \infty$. Given that the eigenvalues of the diagonalized system have opposite signs $\left(\lambda_1 < 0 \text{ and } \lambda_2 > 0\right)$, it is saddle-path stable, with the stable arm corresponding to λ_1. Thus, this special case amounts to the asymptotic growth rates equaling that along the stable arm of the system (25).

This affects the solutions in a particular way. Specifically, if $\theta + \lambda_1 = 0$, the diagonalized equation for A_t is the same as for Equation (SI.3.6) above, but applying the integrating factor $e^{-\lambda_1 t}$ yields

$$\begin{aligned} e^{-\lambda_1 t} y_1'(t) - e^{-\lambda_1 t} \lambda_1 y_1(t) &= -\frac{\lambda_2}{\left(\lambda_2 - \lambda_1\right)} \left(e^{\theta \varphi} \theta t + B_0\right) e^{-(\theta + \lambda_1) t} \\ &= -\frac{\lambda_2}{\left(\lambda_2 - \lambda_1\right)} \left(e^{\theta \varphi} \theta t + B_0\right). \end{aligned} \tag{SI.3.11}$$

Note that there is no exponential term with time as an argument in the last expression. Therefore

$$\int -\frac{\lambda_2}{\left(\lambda_2 - \lambda_1\right)} \left(e^{\theta \varphi} \theta t + B_0\right) dt = -\frac{\lambda_2 e^{\theta \varphi} \theta}{\left(\lambda_2 - \lambda_1\right)} \frac{1}{2} t^2 - \frac{\lambda_2 e^{\theta \varphi} \theta}{\left(\lambda_2 - \lambda_1\right)} B_0 t + C_2 \tag{SI.3.12}$$

and the solution to the differential equation is

$$\begin{aligned} y_1(t) &= -\frac{\lambda_2 e^{\theta \varphi} \theta}{\left(\lambda_2 - \lambda_1\right)} \frac{1}{2} t^2 e^{\lambda_1 t} - \frac{\lambda_2 e^{\theta \varphi} \theta}{\left(\lambda_2 - \lambda_1\right)} B_0 t e^{\lambda_1 t} + C_2 e^{\lambda_1 t} \\ &= -\frac{\lambda_2 e^{\theta \varphi} \theta}{\left(\lambda_2 - \lambda_1\right)} \frac{1}{2} t^2 e^{-\theta t} - \frac{\lambda_2 e^{\theta \varphi} \theta}{\left(\lambda_2 - \lambda_1\right)} B_0 t e^{-\theta t} + C_2 e^{-\theta t} \end{aligned} \tag{SI.3.13}$$

because $\lambda_1 + \theta = 0$ in this case. The solution for $y_2(t)$ is obtained in a similar manner.

In this special case, the solutions to the system in the original coordinates are of the form

$$\begin{aligned} A_t^{Spec} &= \mathrm{A}_1^S e^{-\theta t} t^2 + \mathrm{A}_2^S e^{-\theta t} t + \mathrm{A}_3^S e^{-\theta t} \\ \mathbf{E}_t^{Spec} &= \mathrm{E}_1^S e^{-\theta t} t^2 + \mathrm{E}_2^S e^{-\theta t} t + \mathrm{E}_3^S e^{-\theta t}, \end{aligned} \tag{SI.3.14}$$

where A_i^S's and E_i^S's are again algebraic expressions in the model parameters. These coefficients are different from those in the general case, and the primary structural difference is the presence of the quadratic term.

3.3. Continuity of solutions in parameter space

Given that the system parameters $\alpha, \beta,$ and m can also vary, what we mean more precisely in the preceding discussion is that the condition $\theta + \lambda_1 \neq 0$ does or does not hold given any particular combination (α, β, m). The coefficient expressions in the solutions for the general case (Equation (SI.3.10)) contain the term $\frac{1}{(\theta + \lambda_1)}$, which approaches infinity as θ approaches $-\lambda_1$ in parameter space. The eigenvalues λ_1 and λ_2 are functions of the model parameters $\alpha, \beta, m,$ and δ, and it can be shown that $\theta + \lambda_1 = 0$ is equivalent to

$$\frac{m^2 \beta}{\alpha} = \theta(\theta + \delta). \qquad \text{(SI.3.15)}$$

The parameters θ, φ, and δ are fixed for all versions of the model (θ and φ from the fitted exogenous emissions path and δ as the IPCC conventional value of 0.05). However, our model solutions were a function of m corresponding to different climate models, and we conducted sensitivity analysis with respect to α and β. The difference between the general and special case solutions therefore raises a question of continuity as the parameters of the two solutions approach each other. Using Mathematica we confirmed that the solutions at the parameter configuration (SI. 3.15) are limits of those at nearby points as the parameters approach (SI.3.15), so there is no discontinuity. However, there are additional considerations for numerical solutions, as we discuss next.

3.4. Numerical stability issues.

None of the numerical values used in the cases reported in the text used parameter values that lie exactly on the hypersurface in parameter space defined by (SI.3.15). However, this surface does divide the region in parameter space in which these values lie, and there are numerical issues in the transition between the two cases. Using the general solutions (SI.3.10) in calculations for parameter combinations that are very close to, but not on, the special case gave rise to numerical instabilities because of cumulated rounding errors and the intrinsic precision limits of machine computations. Therefore, it is important to check whether any of the (α, β, m) parameter combinations used in the calculations reported in the text are close enough to satisfying (SI.3.15) that the special case solution needs to be employed rather than the general case in calculating the numerical results. In general, care needs to be taken in numerical implementation of the model to make sure that the correct solutions of the system are the ones employed.

An illustration of the potential problem that could arise from using the general solutions if the parameters are too close to satisfying (SI.3.15) is shown in Fig. S6, a 2-D color plot of the optimal value of the objective function (equation (16) in the text) as a function of β and m. The region with pixels of a color different from the yellow-to-gray shade (which represents values of the objective function) shows the region in which numerical instability is occurring. It can be seen that one of our parameter combinations, m = 0.00286 (Hadley) and β = 0.018 (Nordhaus and Moffat), lies fairly close to the region of numerical instability.

To double-check that this parameter combination is far enough away from satisfying (SI.3.15) to be numerically stable we proceeded as follows. First, we calculated the 18 values of β for which (SI.3.15) is satisfied for the 18 combinations of α and m we used (three α's, six m's). These β's for each (α, m) pair are shown in Table S2. We inspected this table to see which values of β in the Table appeared to be close to one of the β values used in our analysis. For example, the value 0.0183465 associated with the median α and the Hadley m is fairly close to our central β of 0.018. Is it close enough that numerical instability might be a problem affecting the MMR calculations?

To answer this question, we narrowed down the range around the critical value 0.0183465 to see how close one has to be to this value for numerical instability to appear. We then plotted A_t and $\mathbf{E}_t$ for the range $0 \leq t \leq 1000$ over ever-narrowing intervals around this critical value. With increments of 1/10,000,000,000, the plots for A_t over the interval $0.01834649905 \leq \beta \leq 0.01834650395$ are displayed in Fig. S7. (There were 50 incremental steps in this interval given the specified width of each step; the plots for $\mathbf{E}_t$ are similar in appearance.)

What is evident from this figure is that for the first 10 or so steps, the plots of A_t are smoothly well-behaved. After that, the plots begin to get "fuzzy" as the β being used to calculate A_t gets closer to the critical value. From around step 16 through step 35, the numerical instability is more pronounced; beginning with step 22 the numerical calculation of A_t breaks down and even begins showing (theoretically impossible) negative values.

By around step 40, the A_t function becomes well-behaved again, indicating that the value of β is far enough from the critical value that division by a number close enough to zero to cause numerical instability is no longer an issue. Being very conservative, we can conclude that outside the interval, $0.01834649905 \leq \beta \leq 0.01834650395$, the solutions to the model are well-behaved when the general form of the solutions are used. The central value of β used in the calculations reported in the main body of the paper is 0.018, safely outside this interval.

We did a similar analysis for another candidate for instability, $\beta = 0.0241934$, associated with the low α value of 0.000078 and the GFDL m of 0.001572749 and shown in Table S2. This was the critical value closest to our high value of β, which was 0.022. Again, the width of the interval of numerical instability around the critical β value was narrow enough that 0.022 was safely outside of it. Other critical values of β shown in Table S2 are farther away from the values we used than the critical value 0.01834649905 was. We conclude that numerical instability is not a problem for any of the calculations reported in the main body of the paper which were based on the general solutions (SI.3.10).

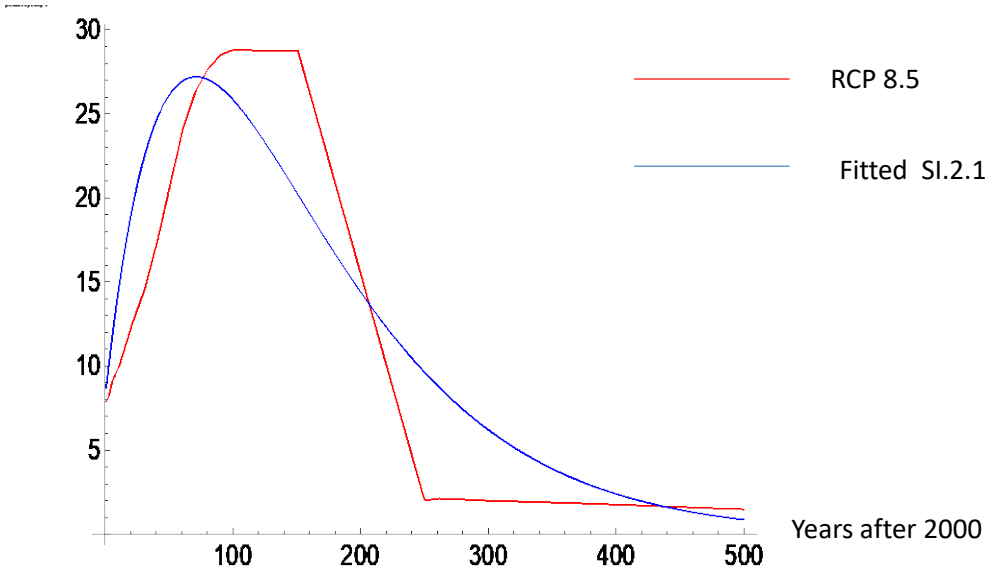

Fig. S1. RCP 8.5 and fitted equation (SI.2.1)

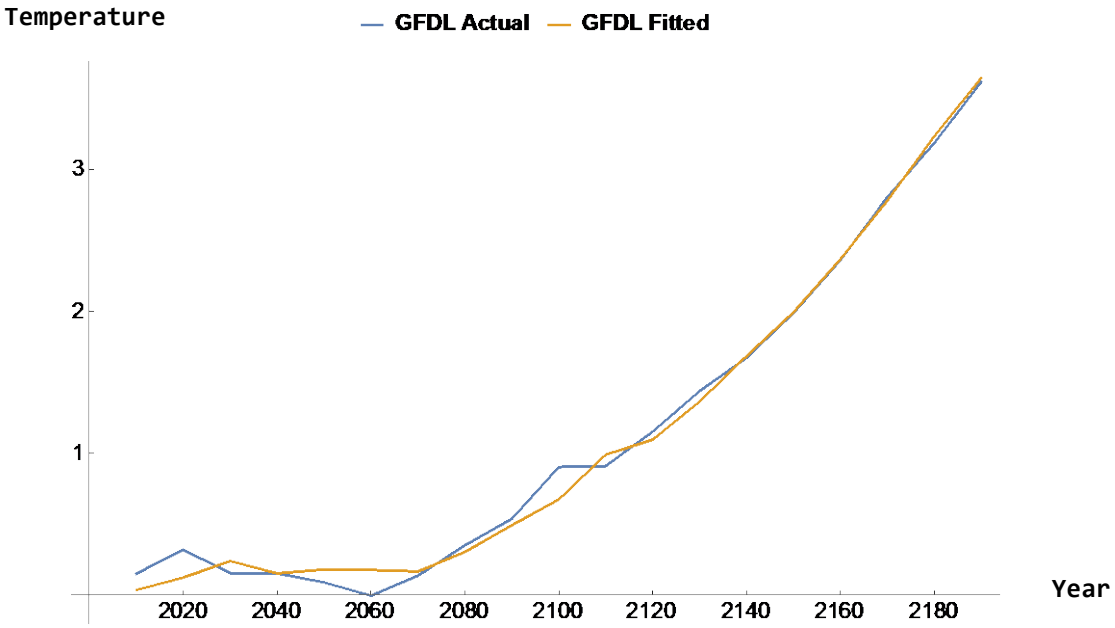

Fig. S2a. GFDL Actual and Fitted

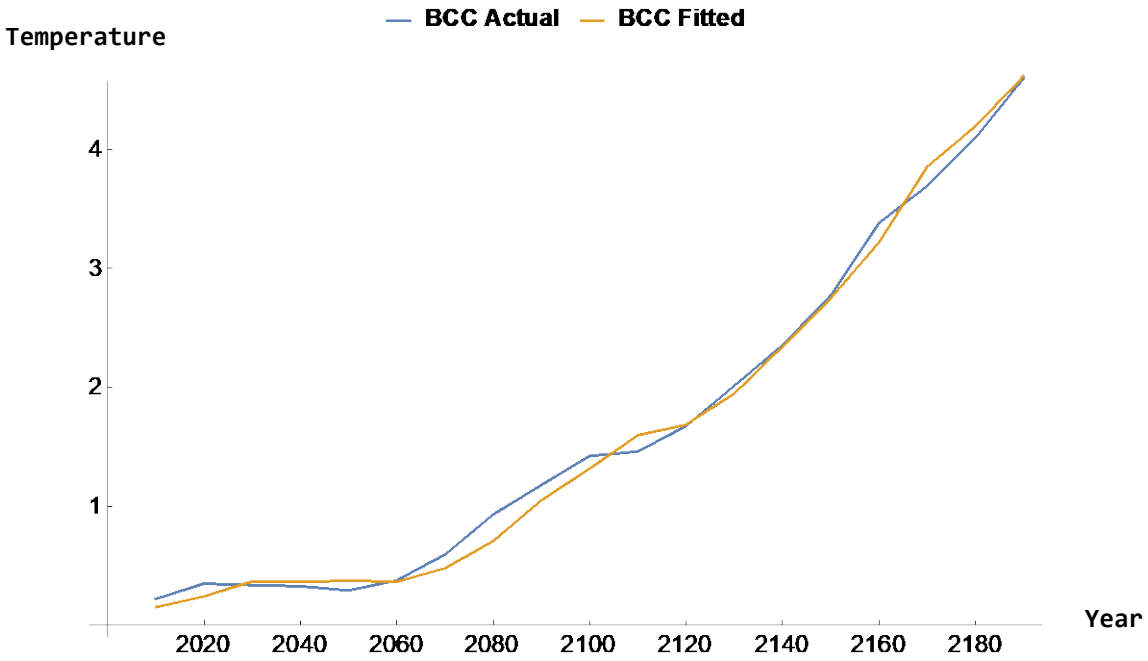

Fig. S2b. BCC Actual and Fitted

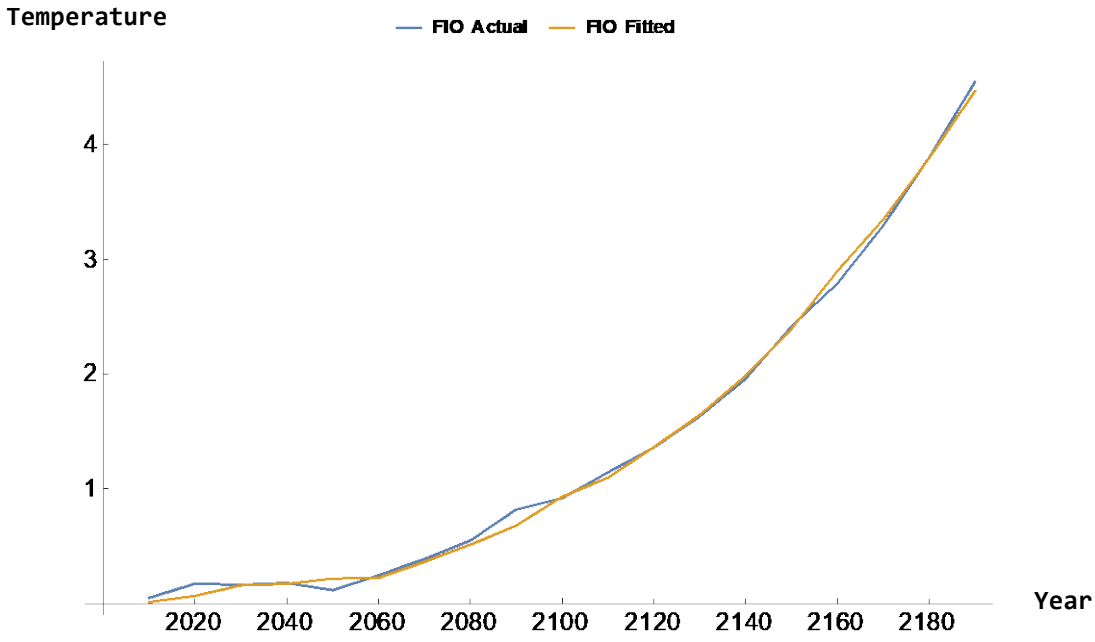

Fig. S2c. FIO Actual and Fitted

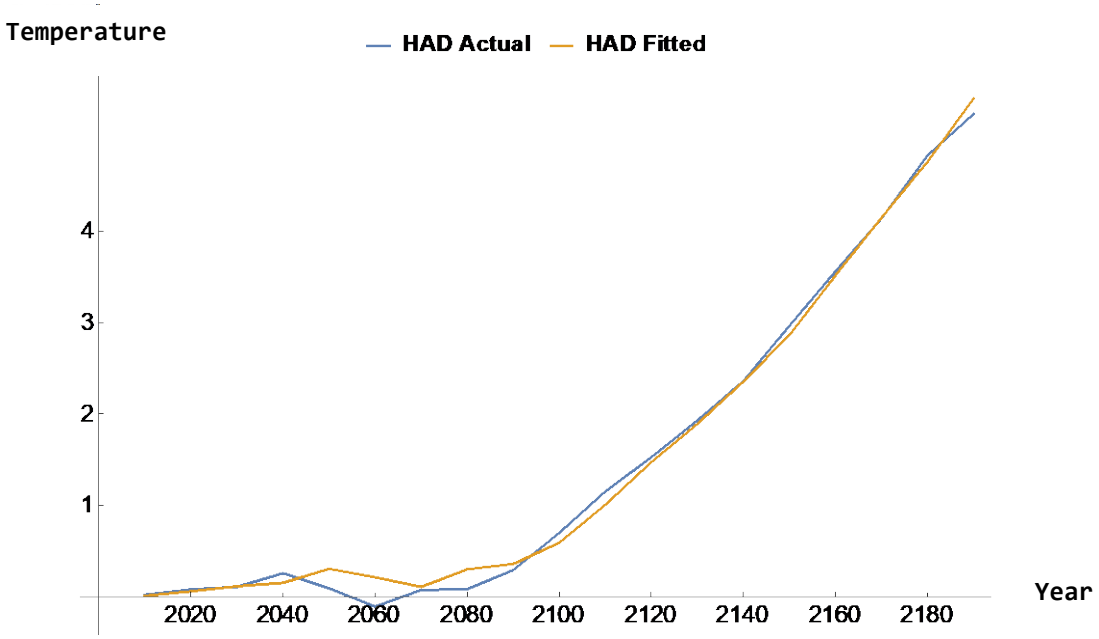

Fig. S2d. Hadley Actual and Fitted

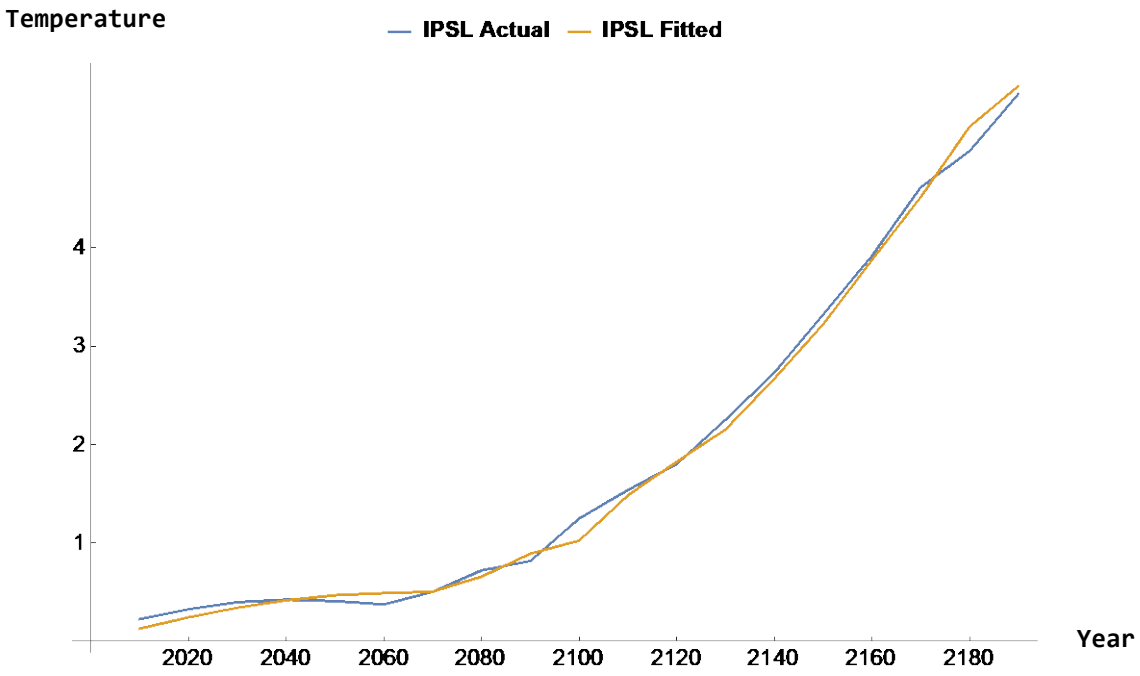

Fig. S2e. IPSL Actual and Fitted

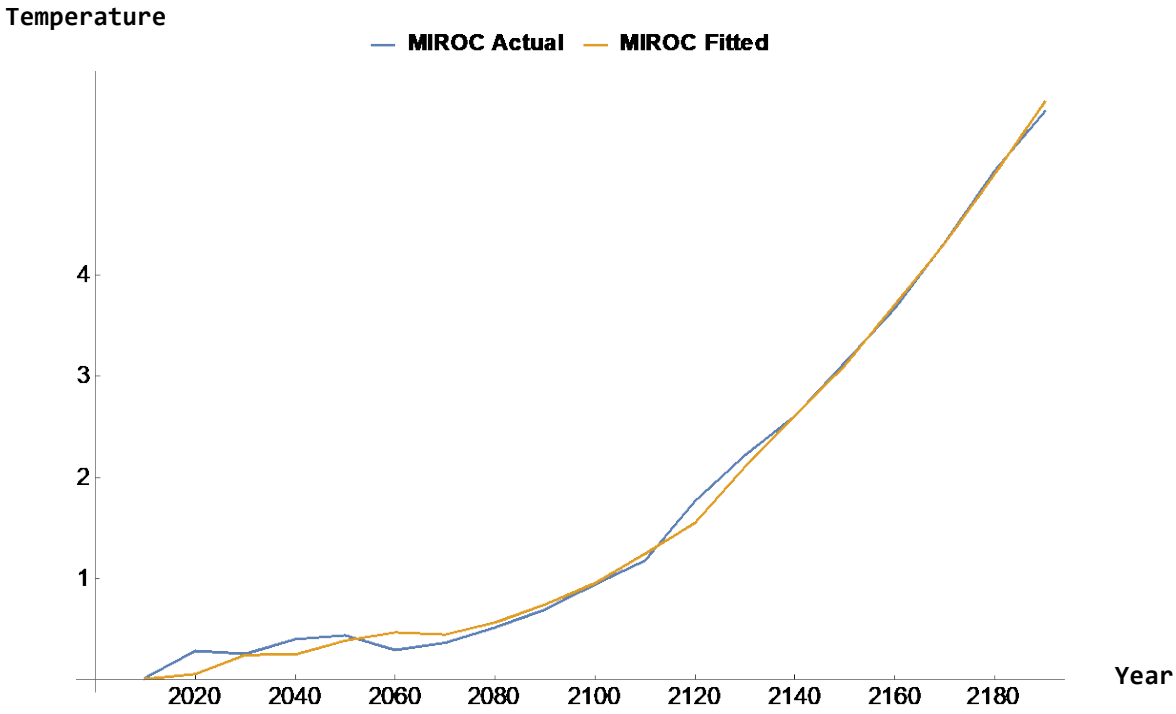

Fig. S2f. MIROC Actual and Fitted

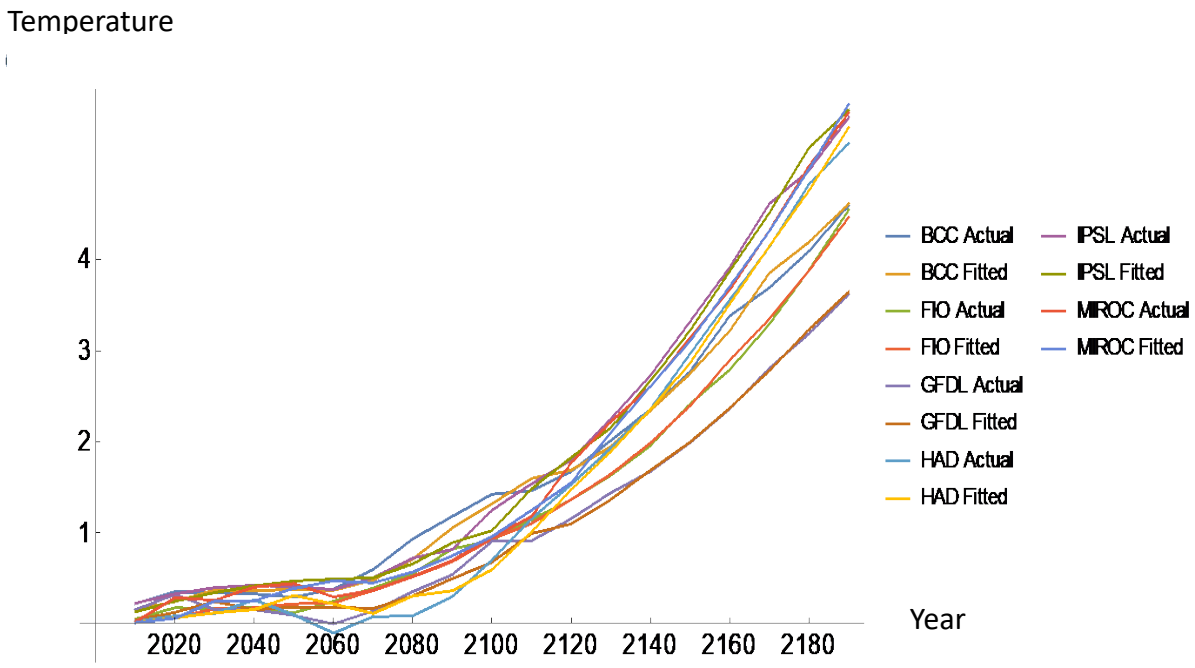

Fig. S3. Actual and Fitted Values from Equation (15), all six models

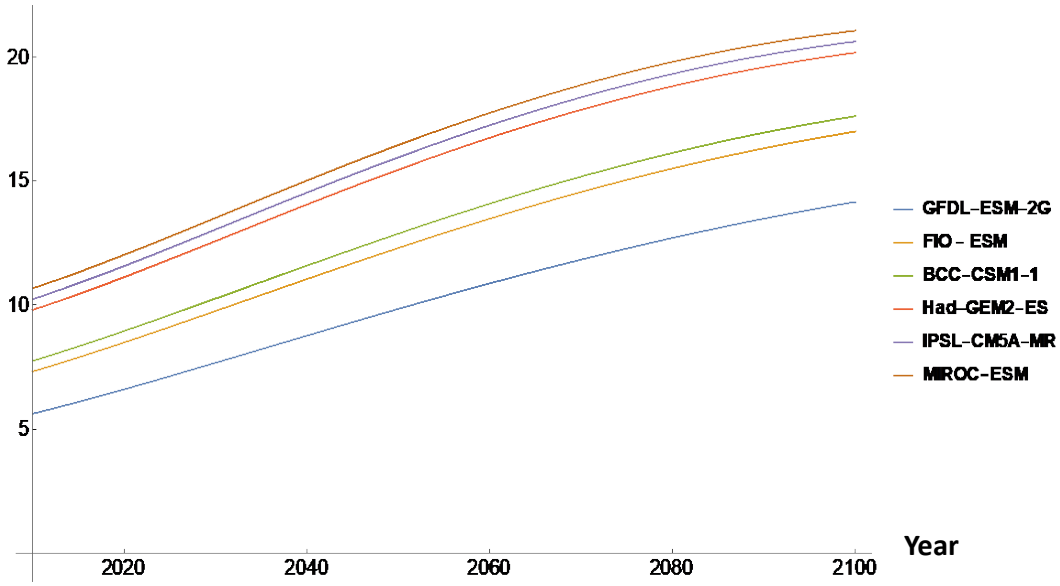

Fig. S4. Optimal Abatement, six ESMs, 2010-2100, α = 0.000125, β = 0.018

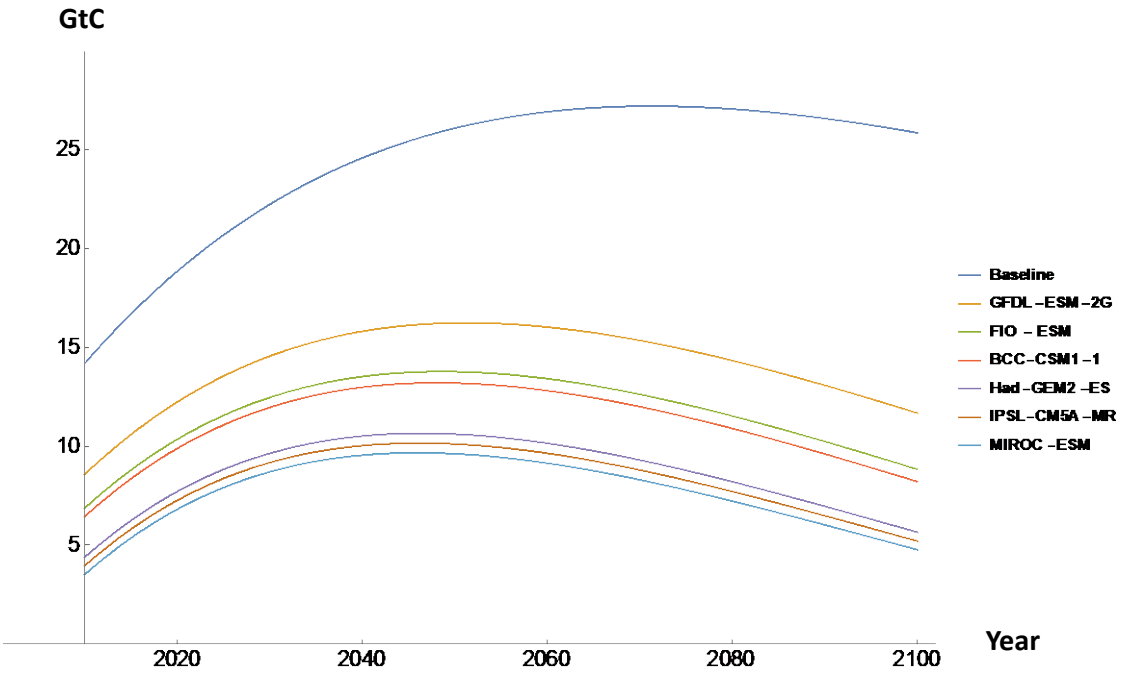

Fig. S5. Baseline (uncontrolled) and net emissions, six ESMs, 2010-2100, α = 0.000125, β = 0.018

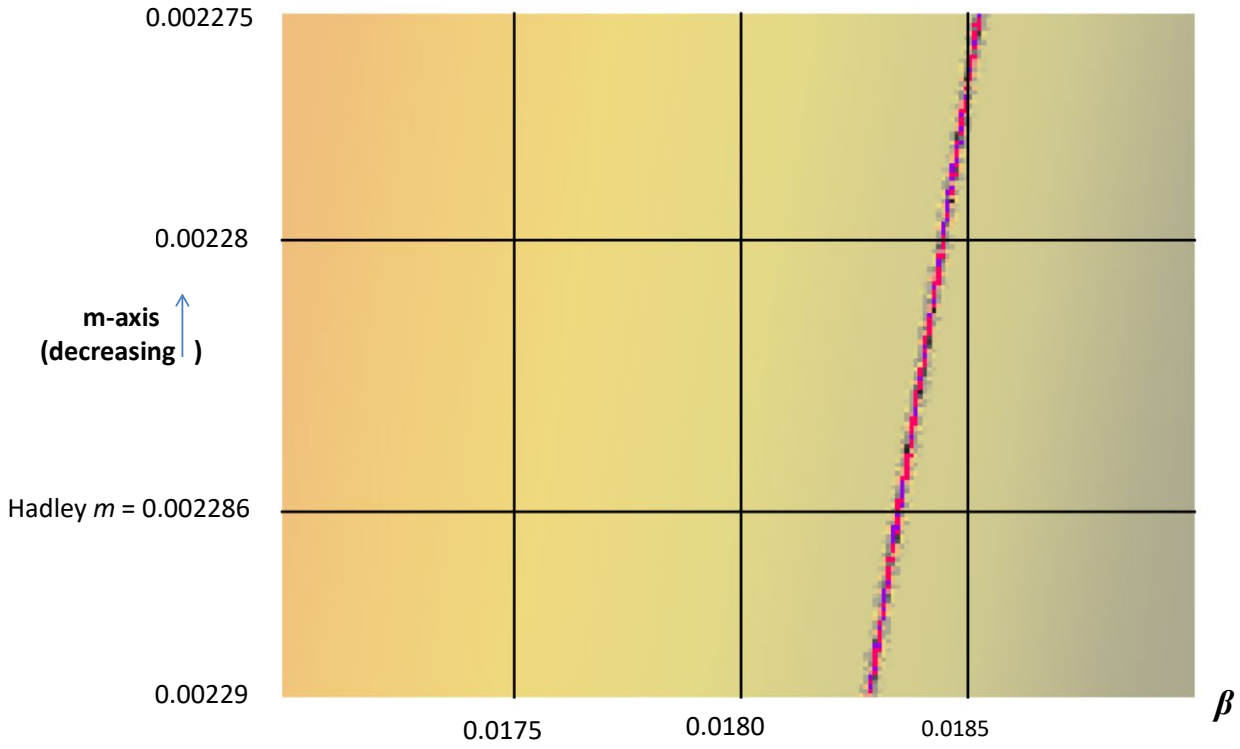

Fig. S6.: 2-D Color Plot of Objective Function,
$\alpha = 0.000125$; $0.017 \leq \beta \leq 0.019$; $0.002275 \leq m \leq 0.002290$

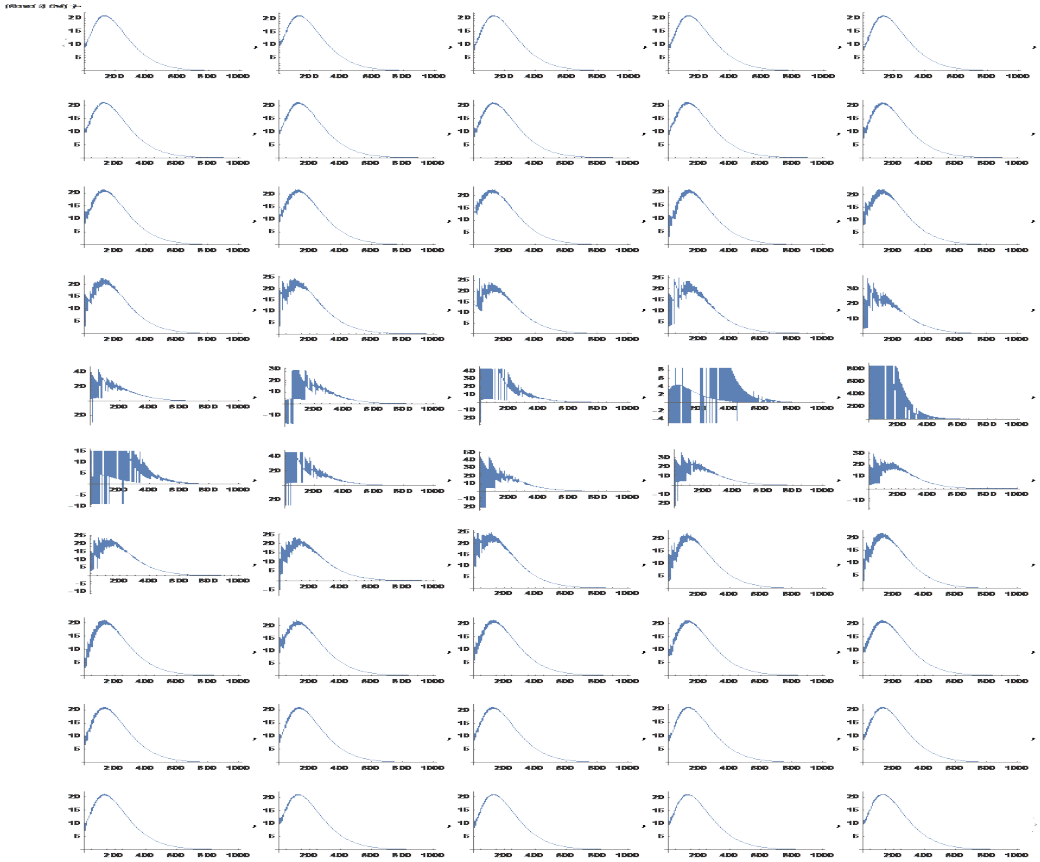

Fig. S7. Numerical instability test on A_t, $0.01834649905 \leq \beta \leq 0.01834650395$, steps of width 1/10,000,000,000

Table S1. Optimal (minimum) costs across values of economic parameters: Present values of abatement costs plus climate damages in optimal solutions.

	***β* Value**								
	Low			Central			High		
	***α* Value**			***α* Value**			***α* Value**		
Model	Low	Median	High	Low	Median	High	Low	Median	High
GFDL-ESM-2G	0.217	0.262	0.301	0.239	0.293	0.343	0.256	0.318	0.377
BCC-CSM1-1	0.279	0.331	0.378	0.315	0.381	0.441	0.343	0.423	0.496
FIO-ESM	0.294	0.348	0.396	0.334	0.403	0.465	0.366	0.450	0.526
Had GEM2-ES	0.367	0.429	0.482	0.427	0.509	0.581	0.479	0.582	0.675
IPSL-CM5A-MR	0.382	0.445	0.500	0.447	0.531	0.605	0.504	0.610	0.706
MIROC-ESM	0.398	0.462	0.518	0.468	0.554	0.630	0.530	0.640	0.739

Table S2. β values for which (SI.3.15) is satisfied, m and α values used for calculations in text

	Model and associated *m* (columns)					
α (rows)	***GFDL*** ***0.001572749***	***BCC*** ***0.00186463***	***FIO*** ***0.001936724***	***Hadley*** ***0.002286328***	***IPSL*** ***0.00236084***	***MIROC*** ***0.002437833***
0.000078	0.241934	0.0172119	0.0159544	0.114482	0.010737	0.0100695
0.000125	0.0387714	0.0275832	0.0254579	0.0183465	0.0172067	0.0161370
0.00020	0.0620342	0.0441332	0.0409086	0.0293544	0.0275307	0.0258192

SI References

1. R. Frisch, Statistical Confluence Analysis by Means of Complete Regression Systems. Oslo, Norway: University Institute for Economics (1934).

2. O. Reiersol, Confluence Analysis by Means of Lag Moments and Other Methods of Confluence Analysis. *Econometrica* 9, 1–24 (1941).

3. S. Klepper, E. Leamer, Consistent Sets of Estimates for Regressions with Errors in All Variables. *Econometrica* 52, 163–183 (1984).

4. J. Horowitz, C. Manski, Identification and Robustness with Contaminated and Corrupted Data. *Econometrica* 63, 281-302 (1995).

5. F. Molinari, Partial Identification of Probability Distributions with Misclassified Data. *J. Econometrics* 144, 81-117 (2008).

6. Duncan, O. and B. Davis, An Alternative to Ecological Correlation. *Am. Sociol. Rev.* 18, 665–666 (1953).

7. L. Rüschendorf, Sharpness of Frechet-Bounds. *Z. Wahrscheinlichkeit*. 57, 293–302 (1981).

8. P. Cross, C. Manski, Regressions, Short and Long. *Econometrica* 70, 357-368 (2002).

9. W. Cochran, F. Mosteller, and J. Tukey, *Statistical Problems of the Kinsey Report on Sexual Behavior in the Human Male* (Washington, DC: American Statistical Association, 1954).

10. C. Manski, Anatomy of the Selection Problem. *J. Human Resour.* 24, 343–360 (1989).

11. C. Manski, *Partial Identification of Probability Distributions* (New York: Springer-Verlag, 2003).

12. C. Manski, *Identification for Prediction and Decision* (Cambridge: Harvard University Press, 2007a).

13. C. Manski, Monotone Treatment Response. Econometrica 65, 1311–1334 (1997).

14. P. Haile, E. Tamer, Inference with an Incomplete Model of English Auctions. *J. Polit. Econ.* 111, 1-51 (2003).

15. F. Ciliberto, E. Tamer, Market Structure and Multiple Equilibria in Airline Markets. *Econometrica* 77, 1791-1828 (2004).

16. C. Manski, Partial Identification of Counterfactual Choice Probabilities. *Int. Econ. Rev.* 48, 1393-1410 (2007b).

17. C. Manski, Identification of Income-Leisure Preferences and Evaluation of Income Tax Policy. *Quant. Econ.* 5, 145-174 (2014).

18. L. Barseghyan, F. Molinari, J. Teitelbaum, Inference under Stability of Risk Preferences. *Quant. Econ.* 7, 367-409 (2016).

19. Wolfram Research, Inc., Wolfram Mathematica 12.1. Champaign, IL (2020).

20. E. Weisstein, Levenberg-Marquardt Method. From MathWorld--
A Wolfram Web Resource. https://mathworld.wolfram.com/Levenberg-MarquardtMethod.html.

21. M. I. A. Lourakis, A Brief Description of the Levenberg-Marquardt Algorithm Implemened{sic] by levmar (2005).
https://www.researchgate.net/publication/239328019_A_Brief_Description_of_the_Levenberg-Marquardt_Algorithm_Implemened by levmar.

22. M. Collins, M. et al., Long-term Climate Change: Projections, Commitments and Irreversibility. In *Climate Change 2013: The Physical Science Basis. Contributions of Working Group I to the Fifth Assessment Report of the Intergovernmental Panel on Climate Change* [Stocker, T. F. et al. (eds.)]. Cambridge University Press, Cambridge, United Kingdom and New York, NY, USA (2013).

23. IHS Global, *EViews11*. Irvine, CA (2020).

24. S. Dietz, F. Venmans, Cumulative carbon emissions and economic policy: In search of general principles. J. Environ. Econ. Manag. 96, 108-129 (2019).

25. R. J. Barro, X. Sala-i-Martin, *Economic Growth* (New York: McGraw Hill, 1995).